Reservoir Stimulation in Petroleum Production

Michael J. Economides, University of Houston
Curtis Boney, Schlumberger Dowell

1-1. Introduction

Reservoir stimulation and artificial lift are the two main activities of the production engineer in the petroleum and related industries. The main purpose of stimulation is to enhance the property value by the faster delivery of the petroleum fluid and/or to increase ultimate economic recovery.

Matrix stimulation and hydraulic fracturing are intended to remedy, or even improve, the natural connection of the wellbore with the reservoir, which could delay the need for artificial lift. This chapter outlines stimulation techniques as tools to help manage and optimize reservoir development.

Understanding stimulation requires understanding the fundamental issues of petroleum production and the position and applicability of the process.

1-1.1. Petroleum production

Petroleum reservoirs are found in geologic formations containing porous rock. Porosity ϕ is the fraction of the rock volume describing the maximum possible fluid volume that can be stored.

Petroleum, often referred to in the vernacular as oil or gas depending on the in-situ conditions of pressure and temperature, is a mixture of hydrocarbons ranging from the simplest, methane, to long-chain hydrocarbons or complex aromatics of considerable molecular weights. Crude oils are frequently referred to as paraffinic or asphaltenic, depending on the dominant presence of compounds within those hydrocarbon families.

The phase behavior of petroleum hydrocarbons is usually greatly simplified, separating compounds in the gaseous phase from those in the liquid phase into two pseudocompounds (oil and gas). The bubble-point pressure p_b of the mixture becomes important. If the reservoir pressure is greater than this value, the fluid is referred to as undersaturated. If the reservoir pressure is below p_b, free gas will form, and the reservoir is known as saturated or two phase. Gas reservoirs exist below the dewpoint pressure.

Petroleum reservoirs also always contain water. The water appears in two forms: within the hydrocarbon zone, comprising the interstitial or connate water saturation S_{wc}, and in underlying water zones, which have different magnitudes in different reservoirs. The connate water saturation is always present because of surface tension and other adhesion affinities between water and rock and cannot be reduced.

The underlying water, segregated from hydrocarbons by gravity, forms a gas-water or oil-water contact that is not sharp and may traverse several feet of formation because of capillary pressure effects. The water may intrude into the hydrocarbon zone as a result of perturbations made during petroleum production.

The ideas of porosity and connate water saturation are coupled with the areal extent of a reservoir A and the reservoir net thickness h to provide the hydrocarbon volume, referred to as initial-oil-in-place or initial-gas-in-place:

$$V_{HC} = Ah\phi(1 - S_{wc}). \qquad (1\text{-}1)$$

Because oil and gas production rates in the petroleum industry are accounted in standard-condition volumes (e.g., standard pressure $p_{sc} = 14.7$ psi or 1 atm [1×10^5 Pa] and standard temperature $T_{sc} = 60°F$ [$15.6°C$]), the right-hand side of Eq. 1-1 is divided by the formation volume factor for oil B_o or for gas B_g.

Wells drilled to access petroleum formations cause a pressure gradient between the reservoir pressure and that at the bottom of the well. During production or injection the pressure gradient forces fluids to flow through the porous medium. Central to this flow is the permeability k, a concept first introduced by Darcy (1856) that led to the well-known Darcy's law. This law suggests that the flow rate q is proportional to the pressure gradient Δp:

$$q \propto k\Delta p. \qquad (1\text{-}2)$$

The fluid viscosity μ also enters the relationship, and for radial flow through an area $2\pi rh$, Eq. 1-2 becomes

$$p - p_{wf} = \frac{q\mu}{2\pi kh} \ln \frac{r}{r_w}, \qquad (1\text{-}3)$$

where p_{wf} and r_w are the bottomhole flowing pressure and wellbore radius, respectively.

Equation 1-3 is also well known and forms the basis to quantify the production (or injection) of fluids through vertical wells from porous media. It is perhaps the most important relationship in petroleum engineering.

The permeability k used in Eq. 1-3 is absolute, implying only one fluid inhabiting and the same fluid flowing through the porous medium. This is, of course, never true for oil or gas flow. In the presence of another fluid, such as connate water, an effective permeability is in force, which is usually symbolized by a subscript (e.g., k_o) and always implied. The effective permeability in a reservoir is smaller than the absolute permeability, which may be measured in a laboratory on cores extracted from the reservoir.

If more than one fluid flows, relative permeabilities that are functions of the fluid saturations are in effect:

$$k_{ro} = \frac{k_o}{k}, \; k_{rw} = \frac{k_w}{k} \text{ and } k_{rg} = \frac{k_g}{k}, \qquad (1\text{-}4)$$

where k_{ro}, k_{rw} and k_{rg} are the relative permeabilities and k_o, k_w and k_g are the effective permeabilities of oil, water and gas, respectively.

Equation 1-3, in conjunction with appropriate differential equations and initial and boundary conditions, is used to construct models describing petroleum production for different radial geometries. These include steady state, where the outer reservoir pressure p_e is constant at the reservoir radius r_e; pseudosteady state, where no flow is allowed at the outer boundary ($q = 0$ at r_e); and infinite acting, where no boundary effects are felt. Well-known expressions for these production modes are presented in the next section.

Regardless of the mode of reservoir flow, the near-well zone may be subjected to an additional pressure difference caused by a variety of reasons, which alters the radial (and horizontal) flow converging into the well.

The skin effect s, which is analogous to the film coefficient in heat transmission, was introduced by Van Everdingen and Hurst (1949) to account for these phenomena. Fundamentally a dimensionless number, it describes a zone of infinitesimal extent that causes a steady-state pressure difference, conveniently defined as

$$\Delta p_s = \frac{q\mu}{2\pi kh} s. \qquad (1\text{-}5)$$

Adding Eqs. 1-3 and 1-5 results in

$$p - p_{wf} = \frac{q\mu}{2\pi kh} \left(\ln \frac{r}{r_w} + s \right), \qquad (1\text{-}6)$$

where the p_{wf} in Eq. 1-6 is different from that in Eq. 1-3. A positive skin effect requires a lower p_{wf}, whereas a negative skin effect allows a higher value for a constant rate q. For production or injection, a large positive skin effect is detrimental; a negative skin effect is beneficial.

Two extensions of Eq. 1-6 are the concepts of effective wellbore radius and the important productivity (or injectivity) index.

With simple rearrangement and employing a basic property of logarithms, Eq. 1-6 yields

$$p - p_{wf} = \frac{q\mu}{2\pi kh} \ln \left(\frac{r}{r_w e^{-s}} \right). \qquad (1\text{-}7)$$

The expression $r_w e^{-s}$ is the effective wellbore radius, denoted as $r_w{}'$. A positive skin effect causes the effective wellbore radius to be smaller than the actual, whereas a negative skin effect has the opposite result.

A second rearrangement yields

$$\frac{q}{p - p_{wf}} = \frac{2\pi kh}{\mu \left[\ln(r_e / r_w) + s \right]} . \qquad (1\text{-}8)$$

The left-hand side of Eq. 1-8 is the well productivity (or injectivity for $p_{wf} > p$) index.

The entire edifice of petroleum production engineering can be understood with this relationship. First, a higher kh product, which is characteristic of particular reservoirs, has a profound impact. The current state of worldwide petroleum production and the relative contributions from various petroleum-producing provinces and countries relate intimately with the kh products of the reservoirs under exploitation. They can range by several orders of magnitude.

There is virtually nothing that a petroleum engineer can do to substantially alter this situation. Mature petroleum provinces imply that following the exploitation of far more prolific zones is the exploitation of increasingly lackluster zones with small kh values, which characterize more recently discovered formations.

A second element of mature fields is reservoir pressure depletion, the effect of which can be seen readily from Eq. 1-8. Although the right-hand side of the equation may be constant, even with a high kh, the production rate q will diminish if $p - p_{wf}$ is reduced. For a constant p_{wf}, reduction in the reservoir pressure p has this effect.

The role of the petroleum production engineer, who must deal with the unalterable kh and pressure of a given reservoir, is to maximize the productivity index by reducing the skin effect and/or the required bottomhole flowing pressure to lift the fluids to the top. Maximizing the productivity index by reducing the skin effect is central to the purpose of this volume and constitutes the notion of stimulation; reducing the bottomhole flowing pressure leads to artificial lift (both gas and pump assisted). Finally, the bottomhole flowing pressure may have an allowable lower limit to prevent or retard undesirable phenomena such as sand production and gas or water coning.

1-1.2. Units

The traditional petroleum engineering oilfield units are not consistent, and thus, most equations that are cast in these units require conversion constants. For example, $1/(2\pi)$ in Eq. 1-3 is appropriate if SI units are used, but must be replaced by the familiar value of 141.2 if q is in STB/D (which must be multiplied also by the formation volume factor B in RB/STB); μ is in cp; h, r and r_w are in ft; and p and p_{wf} are in psi. Table 1-1 contains unit conversion factors for the typical production engineering variables.

For unit conversions there are two possibilities. Either all variables are converted and then two versions of the equation exist (one in oilfield and a second in SI units), or one equation is provided and the result is converted. In this volume the second option is adopted. Generally, the equations are in the traditional oilfield units predominant in the literature.

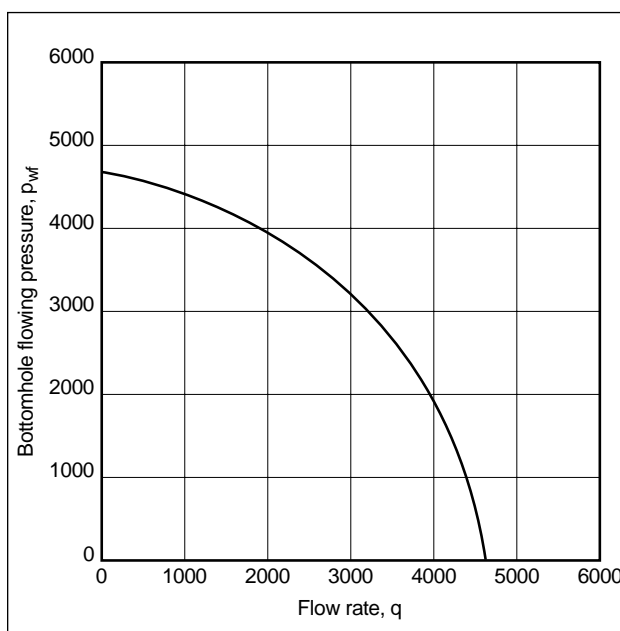| Table 1-1. Unit conversions for petroleum production engineering.			
Variable	Oilfield Units	SI Units	Conversion (multiply oilfield units)
Area, A	ft^2	m^2	9.29×10^{-2}
Compressibility, c_t	psi^{-1}	Pa^{-1}	1.45×10^{-4}
Length	ft	m	3.05×10^{-1}
Permeability, k	md	m^2	9.9×10^{-16}
Pressure, p	psi	Pa	6.9×10^{3}
Rate (oil), q	STB/D	m^3/s	1.84×10^{-6}
Rate (gas), q	Mscf/D	m^3/s	3.28×10^{-4}
Viscosity, μ	cp	Pa-s	1×10^{-3}

Figure 1-1. The inflow performance relationship relates the production rate to the bottomhole flowing pressure.

1-2. Inflow performance

The well production or injection rate is related to the bottomhole flowing pressure by the inflow performance relationship (IPR). A standard in petroleum production, IPR is plotted always as shown in Fig. 1-1.

Depending on the boundary effects of the well drainage, IPR values for steady-state, pseudosteady-state and transient conditions can be developed readily. In the following sections, the relationships for the three main flow mechanisms are presented first for vertical and then for horizontal wells. The

expressions, almost all of which are in wide use, are in oilfield units. A complete outline of their development is in Economides *et al*. (1994).

1-2.1. IPR for steady state

Equation 1-6 can be converted readily to a steady-state expression by simply substituting p with p_e and r with r_e. Thus, in oilfield units and with simple rearrangements, the IPR for oil is

$$q = \frac{kh(p_e - p_{wf})}{141.2B\mu[\ln(r_e/r_w)+s]} . \tag{1-9}$$

A plot of p_{wf} versus q forms a straight line, the vertical intercept is p_e, and the flow rate at the horizontal intercept (i.e., at $p_{wf} = 0$) is known as the absolute open-flow potential. The slope is, of course, constant throughout the production history of the well, assuming single-phase flow, and its value is exactly equal to the reciprocal of the productivity index.

For gas, the analogous expression is approximately

$$q = \frac{kh(p_e^2 - p_{wf}^2)}{1424\overline{\mu}\,\overline{Z}T[\ln(r_e/r_w)+s]} , \tag{1-10}$$

where $\overline{Z}$ is the average gas deviation factor (from ideality), T is the absolute temperature in °R, and $\overline{\mu}$ is the average viscosity.

Equation 1-10 has a more appropriate form using the Al-Hussainy and Ramey (1966) real-gas pseudo-pressure function, which eliminates the need to average μ and Z:

$$q = \frac{kh[m(p_e) - m(p_{wf})]}{1424T[\ln(r_e/r_w)+s]} . \tag{1-11}$$

For two-phase flow, production engineers have used several approximations, one of which is the Vogel (1968) correlation, which generally can be written as

$$\frac{q_o}{q_{o,max}} = 1 - 0.2\frac{p_{wf}}{p} - 0.8\left(\frac{p_{wf}}{p}\right)^2 \tag{1-12}$$

$$q_{o,max} = \frac{AOFP}{1.8} , \tag{1-13}$$

where q_o is the oil production rate, $q_{o,max}$ is the maximum possible oil rate with two-phase flow, and *AOFP* is the absolute open-flow potential of single-phase oil flow.

The usefulness of the Vogel approximation is that it can be used to predict the oil production rate when free gas flows (or is present) although only oil properties are employed. For steady state, Eqs. 1-12 and 1-13 can be combined with Eq. 1-9:

$$q_o = \frac{k_o h p_e\left[1 - 0.2\dfrac{p_{wf}}{p_e} - 0.8\left(\dfrac{p_{wf}}{p_e}\right)^2\right]}{254.2B_o\mu_o[\ln(r_e/r_w)+s]} . \tag{1-14}$$

The subscript o is added here to emphasize the point that oil properties are used. The subscript is frequently omitted, although it is implied. Although neither Eq. 1-11 (for gas) nor Eq. 1-14 (for two-phase flow) provides a straight-line IPR, all steady-state IPRs provide a stationary picture of well deliverability. An interesting group of IPR curves for oil is derived from a parametric study for different skin effects, as shown in Fig. 1-2.
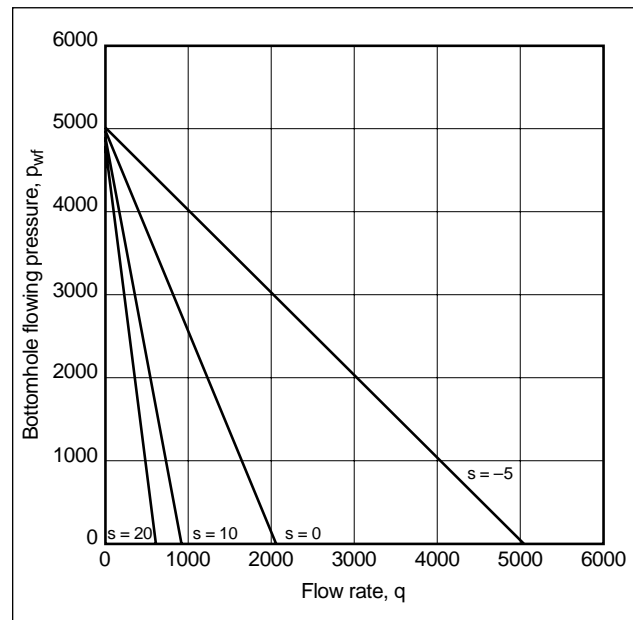

Figure 1-2. *Variation of the steady-state IPR of an oil well for different skin effects.*

- Example of steady-state IPR: skin effect variation

  Suppose that $k = 5$ md, $h = 75$ ft, $p_e = 5000$ psi, $B = 1.1$ RB/STB, $\mu = 0.7$ cp, $r_e = 1500$ ft and $r_w = 0.328$ ft. Develop a family of IPR curves for an undersaturated oil reservoir for skin effects from –5 to 20.

Solution

Using Eq. 1-9 and substituting for the given variables:

$$q = 3.45 \left(\frac{5000 - p_{wf}}{8.43 + s} \right).$$

Figure 1-2 is a plot of the family of IPR curves. For a reasonable $p_{wf} = 2000$, the flow rates at $s = 20$, 0 and –5 are approximately 365, 1230 and 3000 STB/D, respectively, showing the extraordinary impact of a negative skin effect.

1-2.2. IPR for pseudosteady state

At first glance, the expression for pseudosteady-state flow for oil,

$$q = \frac{kh(\bar{p} - p_{wf})}{141.2B\mu[\ln(0.472r_e/r_w) + s]}, \qquad (1\text{-}15)$$

appears to have little difference from the expression for steady state (Eq. 1-9). However, the difference is significant. Equation 1-15 is given in terms of the average reservoir pressure $\bar{p}$, which is not constant but, instead, integrally connected with reservoir depletion.

Material-balance calculations such as the ones introduced by Havlena and Odeh (1963) are required to relate the average reservoir pressure with time and the underground withdrawal of fluids.

Interestingly, the productivity index for a given skin effect is constant although the production rate declines because $\bar{p}$ declines. To stem the decline, the production engineer can adjust the p_{wf}, and thus, artificial lift becomes an important present and future consideration in well management. Successive IPR curves for a well producing at pseudosteady state at different times in the life of the well and the resulting different values of $\bar{p}$ are shown in Fig. 1-3.

The analogous pseudosteady-state expressions for gas and two-phase production are

$$q = \frac{kh[m(\bar{p}) - m(p_{wf})]}{1424T[\ln(0.472r_e/r_w) + s]} \qquad (1\text{-}16)$$

$$q = \frac{kh\bar{p}\left[1 - 0.2\dfrac{p_{wf}}{\bar{p}} - 0.8\left(\dfrac{p_{wf}}{\bar{p}}\right)^2\right]}{254.2B\mu[\ln(0.472r_e/r_w) + s]}. \qquad (1\text{-}17)$$
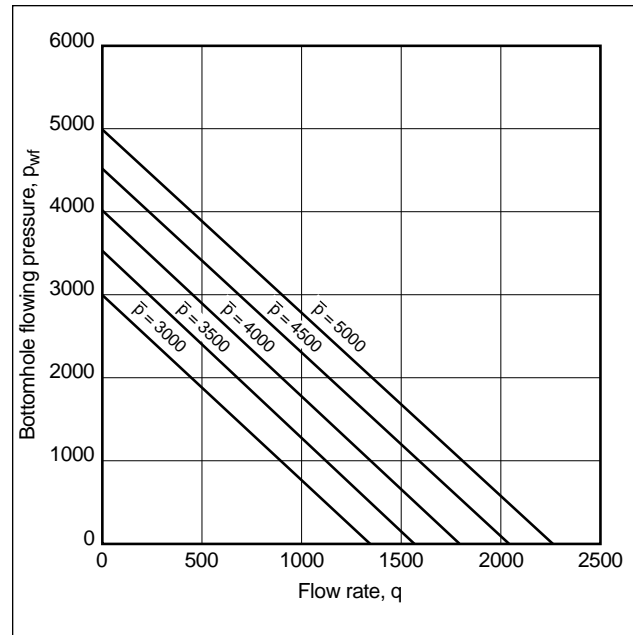

Figure 1-3. *Variation of the pseudosteady-state IPR for an oil well for declining reservoir pressure.*

- Example of pseudosteady-state IPR: effect of average reservoir pressure

  This example repeats the preceding "Example of steady-state IPR: skin effect variation" (page 1-4) for $s = 0$ but allows $\bar{p}$ to vary from 5000 to 3000 in increments of 500 psi.

  Solution

  Using Eq. 1-15 and substituting for the given variables (including $s = 0$):

  $$q = 0.45(\bar{p} - p_{wf}).$$

  In the Fig. 1-3 family of IPR curves for different values of $\bar{p}$, the curves are parallel, reflecting the constant productivity index. (This type of construction assumes that oil remains undersaturated throughout; i.e., above the bubblepoint pressure.)

1-2.3. IPR for transient (or infinite-acting) flow

The convection-diffusion partial differential equation, describing radial flow in a porous medium, is

$$\frac{\partial^2 p}{\partial r^2} + \frac{1}{r}\frac{\partial p}{\partial r} = \frac{\phi \mu c_t}{k}\frac{\partial p}{\partial t}, \qquad (1\text{-}18)$$

where c_t is the total system compressibility, p is pressure, t is time, and r is radial distance. This equation, in wide use in many other engineering fields, provides a well-known solution for an infinite-acting reservoir producing at constant rate at the well.

Using dimensionless variables (for oil, in oilfield units) for pressure and time, respectively:

$$p_D = \frac{kh\Delta p}{141.2qB\mu} \qquad (1\text{-}19)$$

$$t_D = \frac{0.000264kt}{\phi\mu c_t r_w^2} . \qquad (1\text{-}20)$$

For $r = r_w$ (i.e., at the well) a useful approximate form of the solution in dimensionless form is simply

$$p_D = \frac{1}{2}\left(\ln t_D + 0.8091\right). \qquad (1\text{-}21)$$

Equation 1-21 provided the basis of both the forecast of transient well performance and the Horner (1951) analysis, which is one of the mainstays of pressure transient analysis presented in Chapter 2.

Although Eq. 1-21 describes the pressure transients under constant rate, an exact analog for constant pressure exists. In that solution, p_D is replaced simply by the reciprocal of the dimensionless rate $1/q_D$.

The dimensioned and rearranged form of Eq. 1-21, after substitution of the natural log by the log base 10, is

$$q = \frac{kh\left(p_i - p_{wf}\right)}{162.6B\mu}\left(\log t + \log\frac{k}{\phi\mu c_t r_w^2} - 3.23\right)^{-1},$$

$$(1\text{-}22)$$

where p_i is the initial reservoir pressure. The skin effect can be added inside the second set of parentheses as $0.87s$.

As previously done for the pseudosteady-state IPR, gas and two-phase analogs can be written:

$$q = \frac{kh\left[m(p_i) - m(p_{wf})\right]}{1638T}\left(\log t + \log\frac{k}{\phi\mu c_t r_w^2} - 3.23\right)^{-1}$$

$$(1\text{-}23)$$

$$q = \frac{khp_i\left[1 - \dfrac{p_i}{p_{wf}} - \left(\dfrac{p_i}{p_{wf}}\right)^2\right]}{254.2B\mu\left(\log t + \log\dfrac{k}{\phi\mu c_t r_w^2} - 3.23\right)} . \qquad (1\text{-}24)$$

Transient IPR curves can be generated for each instant in time as shown in Fig. 1-4.

- Example of transient IPR

  Using the variables of the previous two examples and $\phi = 0.25$, $c_t = 10^{-5}$ psi^{-1} and $p_i = 5000$ psi, develop transient IPR curves for $t = 3$, 6 and 36 months. The time in Eq. 1-22 must be entered in hours. Assume $s = 0$.

  Solution

  Using Eq. 1-22 and substituting for the given variables:

  $$q = \frac{3\left(5000 - p_{wf}\right)}{\log t + 4.19} .$$

  Figure 1-4 is a graph of the three transient IPRs. The expected flow rate declines for a constant $p_{wf} = 2000$. The flow rates at 3, 6 and 36 months are 1200, 1150 and 1050 STB/D, respectively. The 36-month calculation is unrealistic because it is unlikely that a well would remain infinite acting for such long period of time. Thus, a pseudosteady-state IPR with a $\bar{p}$ intersection at a point below p_i is most likely in effect at that time.

1-2.4. Horizontal well production

Since the mid-1980s horizontal wells have proliferated, and although estimates vary, their share in the
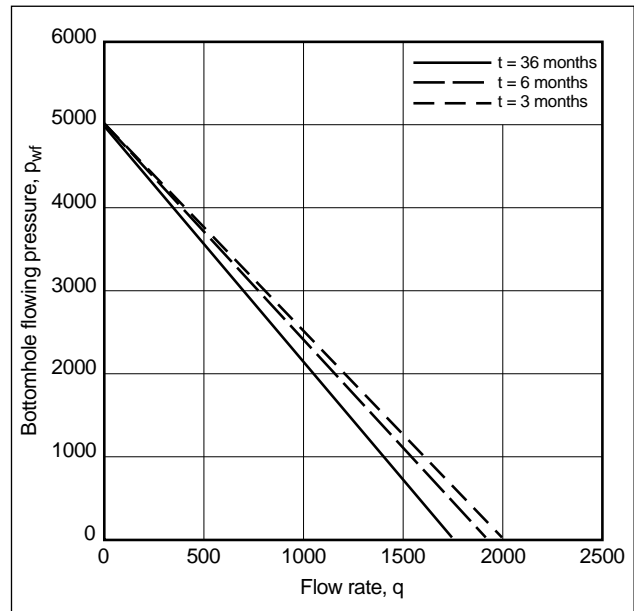

Figure 1-4. Transient IPR curves for an oil well.

production of hydrocarbons will probably reach 50% or more.

A model for a constant-pressure ellipse at steady-state production was introduced by Joshi (1988) and augmented by Economides *et al.* (1991):

$$q = \frac{k_H h (p_e - p_{wf})}{141.2 B\mu \left(\ln\left\{ \frac{\left[a + \sqrt{a^2 - (L/2)^2} \right]}{L/2} \right\} + \frac{I_{ani} h}{L} \ln \frac{I_{ani} h}{\left[r_w (I_{ani} + 1) \right]} \right)} , \quad (1\text{-}25)$$

where L is the horizontal well length and k_H is the horizontal permeability. The latter is the same as that used in all vertical well deliverability relationships. The subscript distinguishes it from the vertical permeability k_V, which is related to the index of the horizontal-to-vertical permeability anisotropy I_{ani}:

$$I_{ani} = \sqrt{\frac{k_H}{k_V}} . \quad (1\text{-}26)$$

The large half-axis a of the horizontal drainage ellipse formed around a horizontal well within an equivalent radius r_{eH} is

$$a = \frac{L}{2} \left\{ 0.5 + \left[0.25 + \left(\frac{r_{eH}}{L/2} \right)^4 \right]^{1/2} \right\}^{1/2} , \quad (1\text{-}27)$$

where r_{eH} is the equivalent radius in a presumed circular shape of a given drainage area. Equation 1-27 transforms it into an elliptical shape.

Equation 1-25 can be used readily to develop a horizontal well IPR and a horizontal well productivity index.

A comparison between horizontal (Eq. 1-25) and vertical (Eq. 1-9) productivity indexes in the same formation is an essential step to evaluate the attractiveness or lack thereof of a horizontal well of a given length over a vertical well. Such comparison generally suggests that in thick reservoirs (e.g., $h > 100$ ft) the index of anisotropy becomes important. The smaller its value (i.e., the larger the vertical permeability), the more attractive a horizontal well is relative to a vertical well. For thinner formations (e.g., $h < 50$ ft), the requirements for good vertical permeability relax.

A skin effect can also be added to the horizontal well deliverability of Eq. 1-25, inside the large

parentheses in the denominator and multiplied by the scaled aspect ratio $I_{ani}h/L$.

For gas and two-phase flow, Eq. 1-25 can be adjusted readily by the transformations (compared with Eq. 1-9) shown in Eqs. 1-11 and 1-14.

For pseudosteady state, a generalized horizontal well production model, accounting for any positioning of a well laterally and vertically within a drainage, was presented by Economides *et al.* (1996). The basic model in Fig. 1-5 has reservoir dimensions x_e, y_e and h, horizontal well length L and an angle φ between the well projection on the horizontal plane and x_e.
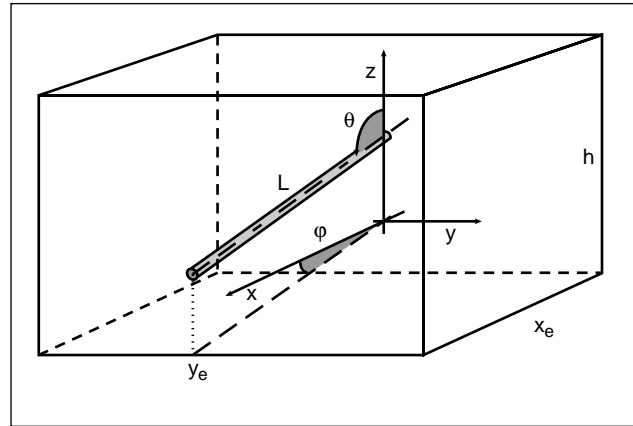

Figure 1-5. Generalized well model for production from an arbitrarily oriented well in an arbitrarily shaped reservoir (Economides et al., 1996).

The solution is general. First, the pseudosteady-state productivity index J is used:

$$J = \frac{q}{\bar{p} - p_{wf}} = \frac{k x_e}{887.22 B\mu \left(p_D + \frac{x_e}{2\pi L \sum s} \right)} , \quad (1\text{-}28)$$

where the reservoir permeability k is assumed to be isotropic throughout (it is adjusted later) and x_e is the well drainage dimension. The constant allows the use of oilfield units; the productivity index is in STB/D/psi. The summation of the skin effects Σs accounts for all damage and mechanical skin effects. Finally, the dimensionless pressure is

$$p_D = \frac{x_e C_H}{4\pi h} + \frac{x_e}{2\pi L} s_x . \quad (1\text{-}29)$$

Equation 1-29 decomposes a three-dimensional (3D) problem into one two-dimensional term and one one-dimensional term. The first term on the right-hand side accounts for horizontal positioning effects, with C_H as a shape factor. The second term accounts for both the reservoir thickness (causing a distortion of the flow lines) and the additional effects from vertical eccentricity in the case that the well is not positioned at the vertical middle of the reservoir.

The vertical effects skin effect s_x is (after Kuchuk *et al.*, 1988)

$$s_x = \ln\left(\frac{h}{2\pi r_w}\right) - \frac{h}{6L} + s_e , \qquad (1\text{-}30)$$

where s_e is the vertical eccentricity skin:

$$s_e = \frac{h}{L}\left[\frac{2z_w}{h} - \frac{1}{2}\left(\frac{2z_w}{h}\right)^2 - \frac{1}{2}\right] - \ln\left[\sin\left(\frac{\pi z_w}{h}\right)\right],$$

$$(1\text{-}31)$$

where z_w is the elevation from the bottom of the reservoir. For a well at the vertical middle, $s_e = 0$.

- Example calculation of s_x for two thicknesses

  Assume that $L = 2000$ ft and $r_w = 0.328$ ft. Calculate s_x for $h = 50$ ft and $h = 200$ ft.

  Solution

  Using Eq. 1-30 for $h = 50$ ft:

$$s_x = \ln\frac{50}{(2)(3.14)(0.328)} - \frac{50}{(6)(2000)} = 3.2 .$$

For $h = 200$ ft, $s_x = 4.6$. This calculation suggests that for thicker reservoirs the distortion of the flowlines has relatively more severe detrimental effects.

Figure 1-6 provides values for s_x for a range of reservoir thicknesses and a centered well ($r_w = 0.4$ ft).

For the case of a vertically eccentered well, Fig. 1-7 provides values for s_e for various levels of eccentricity. The values in Fig. 1-7 are the same for symmetrical eccentricity; i.e., s_e is the same for $z_w/h = 0.1$ and 0.9. At $z_w/h = 0.5$, $s_e = 0$, as expected.

To account for the position of the well in the horizontal plane, a series of shape factors is presented in Table 1-2. Although the solution pre-
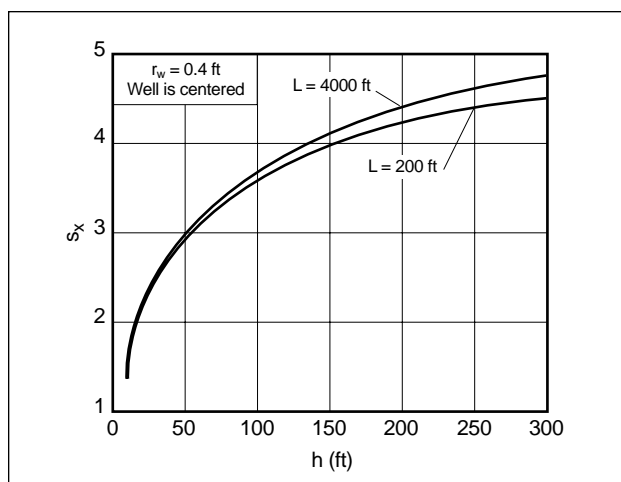

Figure 1-6. *Vertical effects skin effect for a horizontal well (Economides* et al*., 1996).*
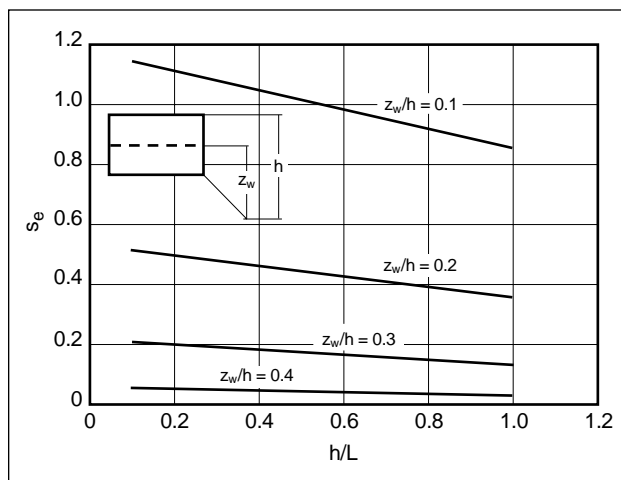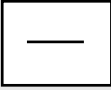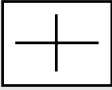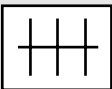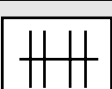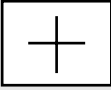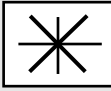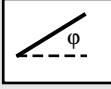

Figure 1-7. *Vertical eccentricity skin effect (Economides* et al*., 1996).*
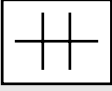
sented by Economides *et al.* (1996) is general and a computer program is available, the library of shape factors in Table 1-2 is useful for quick approximations (in the style of the classic Dietz [1965] factors for vertical wells). Multiple horizontal well configurations are also included.

- Example calculation of horizontal well productivity index: comparison with a vertical well

  Assume that $L = 2000$ ft, $x_e = y_e = 2700$ ft, $h = 200$ ft, $r_w = 0.328$ ft, $B = 1$ RB/STB and $\mu = 1$ cp. The well is in the vertical middle (i.e., $s_e = 0$). Permeability $k = 10$ md. For this example, the productivity index is calculated for an isotropic reservoir. However, the permeability of most reservoirs is not isotropic between the vertical and horizontal planes, resulting in a consid-

Table 1-2. Shape factors for well productivity (Economides *et al.*, 1996).							
		L/x_e	C_H				C_H
(diagram)	$x_e = 4y_e$	0.25	3.77	(diagram)	$x_e = y_e$ $L_x/x_e = 0.4$	$L_y = 2L_x$ $L_y = L_x$ $L_y = 0.5L_x$	1.10 1.88 2.52
		0.5	2.09				
		0.75	1.00				
		1	0.26				
(diagram)	$x_e = 2y_e$	0.25	3.19	(diagram)	$x_e = y_e$ $L_x/x_e = 0.4$	$L_y = 2L_x$ $L_y = L_x$ $L_y = 0.5L_x$	0.79 1.51 2.04
		0.5	1.80				
		0.75	1.02				
		1	0.52				
(diagram)	$x_e = y_e$	0.25	3.55	(diagram)	$x_e = y_e$ $L_x/x_e = 0.4$	$L_y = 2L_x$ $L_y = L_x$ $L_y = 0.5L_x$	0.66 1.33 1.89
		0.4	2.64				
		0.5	2.21				
		0.75	1.49				
		1	1.04				
(diagram)	$2x_e = y_e$	0.25	4.59	(diagram)	$x_e = y_e$ $L_x/x_e = 0.4$	$L_y = 2L_x$ $L_y = L_x$ $L_y = 0.5L_x$	0.59 1.22 1.79
		0.5	3.26				
		0.75	2.53				
		1	2.09				
(diagram)	$4x_e = y_e$	0.25	6.69				
		0.5	5.35				
		0.75	4.63				
		1	4.18				
(diagram)	$x_e = y_e$	0.25	2.77				
		0.5	1.47				
		0.75	0.81				
		1	0.46				
(diagram)	$x_e = y_e$	0.25	2.66				
		0.5	1.36				
		0.75	0.69				
		1	0.32				
(diagram)	$x_e = y_e$ $L/x_e = 0.75$	0	1.49				
		30	1.48				
		45	1.48				
		75	1.49				
		90	1.49				

erable reduction in the productivity index, as shown in the next section.

Solution

From the "Example calculation of s_x for two thicknesses" (page 1-8), $s_x = 4.6$, and from Table 1-2 for $x_e = y_e$ and $L/x_e = 2000/2700 \approx 0.75$, $C_H = 1.49$.

Using Eq. 1-29:

$$p_D = \frac{(2700)(1.49)}{(4)(3.14)(200)} + \frac{(2700)(4.6)}{(2)(3.14)(2000)} = 2.59,$$

and using Eq. 1-28:

$$J_H = \frac{(10)(2700)}{(887.22)(1)(1)(2.59)} = 11.7 \text{ STB} / \text{D} / \text{psi}.$$

The productivity index of a vertical well in the same formation, under pseudosteady-state conditions and assuming that the well is in the center of the square reservoir, is

$$J_V = \frac{kh}{141.2B\mu \, \ln(0.472r_e \, / \, r_w)}.$$

The drainage area is 2700×2700 ft, resulting in $r_e = 1520$ ft. Thus,

$$J_V = \frac{(10)(200)}{(141.2)(1)(1)\ln[(0.472)(1520)/(0.328)]}$$

$$= 1.84 \text{ STB} / \text{D} / \text{psi}.$$

The productivity index ratio between a horizontal and a vertical well in this permeability-isotropic formation is $11.7/1.84 = 6.4$.

1-2.5. Permeability anisotropy

From dealing with vertical wells, petroleum engineers learned to generally ignore the concept of permeability anisotropy and refer to reservoirs as having permeabilities equal to 0.1, 3, 100 md, etc., as if permeability were a scalar quantity.

Although it has been known for a long time that permeability has different values in different directions (i.e., it is a vector) and although the impact of such anisotropy is recognized in waterflooding and even in the spacing of wells, for production from a single vertical well it is of little concern. Muskat (1937), in one of his many early contributions, suggested that the permeability affecting vertical well production is

$$\bar{k} = \bar{k}_H = \sqrt{k_x k_y}, \qquad (1\text{-}32)$$

where $\bar{k}$ is the average permeability, which for a vertical well is equal to the average horizontal permeability $\bar{k}_H$, and k_x and k_y are the permeabilities in the x and y directions, respectively.

Although the "average" permeability in Eq. 1-32 could equal 10 md, this value could result because the permeabilities in the x direction and y direction are both equal to 10 md or because $k_x = 100$ md and $k_y = 1$ md. Horizontal-to-horizontal permeability anisotropy of such magnitude is rare. However, permeability anisotropies in the horizontal plane of 3:1 and higher are common (Warpinski, 1991). Logically, a horizontal well drilled normal to the maximum rather than the minimum permeability should be a better producer.

Suppose all permeabilities are known. Then the horizontal well length, wellbore radius and reservoir dimensions can be adjusted. These adjusted variables, presented by Besson (1990), can be used instead of the true variables in predicting well performance with the model in Section 1-2.4:

Length: $\qquad L' = L\alpha^{-1/3}\beta \qquad (1\text{-}33)$

Wellbore radius: $\qquad r_w' = r_w \dfrac{\alpha^{2/3}}{2}\left(\dfrac{1}{\alpha\beta}+1\right), \qquad (1\text{-}34)$

where

$$\alpha = \sqrt{\frac{\left(k_x k_y\right)^{1/2}}{k_z}} \qquad (1\text{-}35)$$

$$\beta = \left(\sqrt{\frac{k_y}{k_x}}\cos^2\varphi + \sqrt{\frac{k_x}{k_y}}\sin^2\varphi\right)^{1/2} \qquad (1\text{-}36)$$

$$x' = x\frac{\sqrt{k_y k_z}}{\bar{k}} \qquad (1\text{-}37)$$

$$y' = y\frac{\sqrt{k_x k_z}}{\bar{k}} \qquad (1\text{-}38)$$

$$z' = z\frac{\sqrt{k_x k_y}}{\bar{k}} \qquad (1\text{-}39)$$

$$\bar{k} = \sqrt[3]{k_x k_y k_z}. \qquad (1\text{-}40)$$

- Example of horizontal well productivity index in an anisotropic reservoir

Repeat the calculations in "Example calculation of horizontal well productivity index: comparison with a vertical well" (page 1-8) but with $k_x = 20$ md, $k_y = 5$ md (the average horizontal permeability is still 10 md) and $k_z = 1$ md. Assume that the well is parallel to the x_e boundary; i.e., the angle $\varphi = 0$.

Solution

From Eqs. 1-35 and 1-36, $\alpha = 3.16$ and $\beta = 0.707$, respectively. The horizontal well length is then adjusted using Eq. 1-33 and becomes 964 ft. The wellbore radius is adjusted using Eq. 1-34 and becomes 0.511 ft. The reservoir dimensions x_e, y_e and h are adjusted using Eqs. 1-37 through 1-39 and become 1304, 2608 and 432 ft, respectively.

The vertical effect skin effect from Eq. 1-30 is 4.85. The adjusted reservoir dimensions become $2x_e = y_e$. The adjusted penetration ratio L/x_e remains the same (0.75). Thus, from Table 1-2 the shape factor is 2.53.

Using Eq. 1-29 for dimensionless pressure and substituting with the adjusted variables:

$$p_D = \frac{(1304)(2.53)}{(4)(3.14)(432)} + \frac{(1304)(4.85)}{(2)(3.14)(964)} = 1.65,$$

and using Eq. 1-28, the productivity index becomes

$$J = \frac{(4.63)(1304)}{(887.22)(1)(1)(1.65)} = 4.12 \text{ STB} / \text{D} / \text{psi},$$

representing a 65% reduction from the value of 11.7 STB/D/psi calculated in the preceding "Example calculation of horizontal well productivity index: comparison with a vertical well" for the isotropic case.

1-3. Alterations in the near-wellbore zone

The skin effect *s* is intended to describe alterations in the near-wellbore zone. One of the most common problems is damage to the permeability that can be caused by practically any petroleum engineering activity, from drilling to well completions to stimulation itself. As mentioned in Section 1-1.1, the skin effect is a dimensionless number that can be obtained from a well test, as explained in detail in Chapter 2.

The nature of radial flow is that the pressure difference in the reservoir increases with the logarithm of distance; i.e., the same pressure is consumed within the first foot as within the next ten, hundred, etc. If the permeability of the near-wellbore zone is reduced significantly it is entirely conceivable that the largest portion of the total pressure gradient may be consumed within the very near wellbore zone. Similarly, recovering or even improving this permeability may lead to a considerable improvement in the well production or injection. This is the role of matrix stimulation.

1-3.1. Skin analysis

Figure 1-8 describes the areas of interest in a well with an altered zone near the wellbore. Whereas *k* is the "undisturbed" reservoir permeability, k_s is the permeability of this altered zone.

The Van Everdingen and Hurst (1949) skin effect has been defined as causing a steady-state pressure difference (Eq. 1-5). Skin effect is mathematically dimensionless. However, as shown in Fig. 1-8, it reflects the permeability k_s at a distance r_s. A relationship among the skin effect, reduced permeability and altered zone radius may be extracted. Assuming
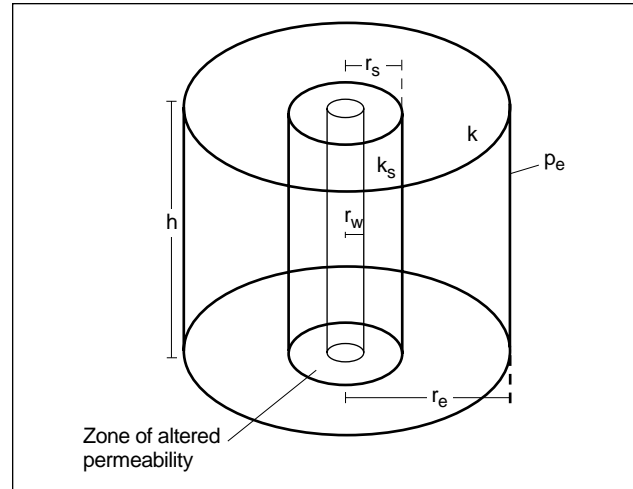
Figure 1-8. *Zone of altered permeability* k_s *near a well.*

that p_s is the pressure at the outer boundary of the altered zone, from Eq. 1-9 the undamaged relation is

$$q = \frac{kh\left(p_s - p_{wf,ideal}\right)}{141.2 B\mu \ln \dfrac{r_s}{r_w}}, \tag{1-41}$$

and if damaged,

$$q = \frac{k_s h\left(p_s - p_{wf,real}\right)}{141.2 B\mu \ln \dfrac{r_s}{r_w}}, \tag{1-42}$$

using the respective values of undamaged ideal and damaged real bottomhole flowing pressure.

Equations 1-41 and 1-42 may be combined with the definition of skin effect and the obvious relationship

$$\Delta p_s = p_{wf,ideal} - p_{wf,real} \tag{1-43}$$

to obtain

$$\Delta p_s = \frac{141.2 qB\mu}{h} \ln\left(\frac{r_s}{r_w}\right)\left(\frac{1}{k_s} - \frac{1}{k}\right). \tag{1-44}$$

Equations 1-44 and 1-5 can then be combined:

$$s = \left(\frac{k}{k_s} - 1\right)\ln\frac{r_s}{r_w}, \tag{1-45}$$

which is the sought relationship. This is the well-known Hawkins (1956) formula.

Equation 1-45 leads to one of the best known concepts in production engineering. If $k_s < k$, the well is damaged and $s > 0$; conversely, if $k_s > k$, then $s < 0$ and the well is stimulated. For $s = 0$, the near-wellbore permeability is equal to the original reservoir permeability.

Certain well logs may enable calculation of the damaged radius, whereas pressure transient analysis may provide the skin effect and reservoir permeability. Equation 1-45 may then provide the value of the altered permeability k_s.

Frick and Economides (1993) postulated that in the absence of production log measurements, an elliptical cone is a more plausible shape of damage distribution along a horizontal well. A skin effect expression, analogous to the Hawkins formula, was developed:

$$s_{eq} = \left(\frac{k}{k_s} - 1\right) \ln\left[\frac{1}{I_{ani} + 1}\sqrt{\frac{4}{3}\left(\frac{a_{sH,max}^2}{r_w^2} + \frac{a_{sH,max}}{r_w} + 1\right)}\right],$$

(1-46)

where I_{ani} is the index of anisotropy and $a_{sH,max}$ is the horizontal axis of the maximum ellipse, normal to the well trajectory. The maximum penetration of damage is near the vertical section of the well. The shape of the elliptical cross section depends greatly on the index of anisotropy.

The skin effect s_{eq} is added to the second logarithmic term in the denominator of the horizontal well production expression (Eq. 1-25) and must be multiplied by $I_{ani}h/L$. One obvious, although not necessarily desirable, way to offset the effects of damage is to drill a longer horizontal well.

1-3.2. Components of the skin effect

Matrix stimulation has proved to be effective in reducing the skin effect caused by most forms of damage. However, the total skin effect is a composite of a number of factors, most of which usually cannot be altered by conventional matrix treatments. The total skin effect may be written as

$$s_t = s_{c+\theta} + s_p + s_d + \sum pseudoskins.$$ (1-47)

The last term in the right-hand side of Eq. 1-47 represents an array of pseudoskin factors, such as phase-dependent and rate-dependent effects that could be altered by hydraulic fracturing treatments. The other three terms are the common skin factors. The first is the skin effect caused by partial completion and slant. It has been well documented by Cinco-Ley *et al.* (1975a). The second term represents the skin effect resulting from perforations, as described by Harris (1966) and expounded upon by Karakas and Tariq (1988). The third term refers to the damage skin effect.

Obviously, it is of extreme importance to quantify the components of the skin effect to evaluate the effectiveness of stimulation treatments. In fact, the pseudoskin effects can overwhelm the skin effect caused by damage. It is not inconceivable to obtain skin effects after matrix stimulation that are extremely large. This may be attributed to the usually irreducible configuration skin factors.

1-3.3. Skin effect caused by partial completion and slant

Figure 1-9 is relevant to Cinco-Ley *et al.*'s (1975a) development. Table 1-3 presents the pseudoskin factors caused by partial penetration and slant. To use them, it is necessary to evaluate several dimensionless groups:

Completion thickness	$h_{wD} = h_w/r_w$	(1-48)
Elevation	$z_{wD} = z_w/r_w$	(1-49)
Reservoir thickness	$h_D = h/r_w$	(1-50)
Penetration ratio	$h_{wD}' = h_w/h.$	(1-51)

The terms h_D, h_{wD}, z_{wD}/h_D and $h_{wD}\cos\theta/h_D$ must be known to evaluate the skin effect.

As an example, assume $h_D = 100$, $z_{wD}/h_D = 0.5$ (midpoint of the reservoir) and $h_{wD}\cos\theta/h_D = 0.25$ ($\theta = 60°$, $h_w/h = 0.5$). For this case, $s_{c+\theta} = 5.6$ (from Table 1-3). If the penetration ratio is reduced to 0.1, the skin effect increases to 15.5.

It is apparent that this skin effect alone could dwarf the skin effect caused by damage. The skin effect resulting from the partial penetration length h_{wD}' may be unavoidable because it typically results from other operational considerations (such as the prevention of gas coning).

From Table 1-3 and for full penetration it can be seen readily that a deviated well, without damage, should have a negative skin effect. Thus, a small skin effect or even one equal to zero obtained from
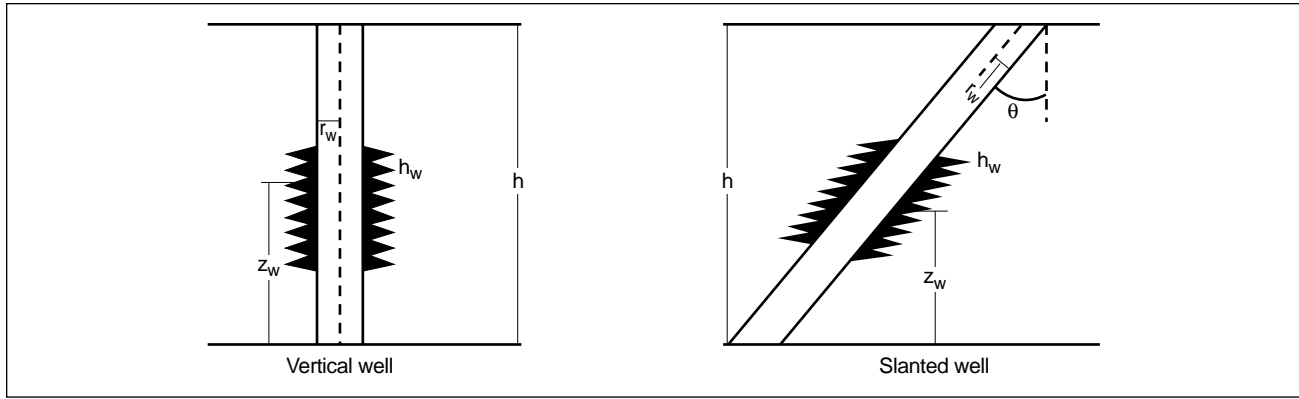
Figure 1-9. *Geometry for partial and off-centered completions and slant skin effects (Cinco-Ley et al., 1975a).*

a well test in a highly deviated well may mean considerable damage. Removal of this damage with appropriate stimulation could increase the deviated well production (or injection) considerably.

1-3.4. Perforation skin effect

Karakas and Tariq (1988) developed a procedure to calculate the skin effect caused by perforations. This skin effect is a composite involving the plane-flow effect s_H, vertical converging effect s_V and wellbore effect s_{wb}:

$$s_p = s_H + s_V + s_{wb}. \qquad (1\text{-}52)$$

The pseudoskin factor s_H is given by

$$s_H = \ln \frac{r_w}{r_w'(\theta)}, \qquad (1\text{-}53)$$

where $r_w'(\theta)$ is the effective wellbore radius and is a function of the perforation phasing angle θ:

$$r_w'(\theta) = \begin{cases} l_p/4 & \text{when } \theta = 0 \\ \alpha_\theta(r_w + l_p) & \text{when } \theta \neq 0 \end{cases}, \qquad (1\text{-}54)$$

where l_p is the length of the perforation and α_θ is a phase-dependent variable and can be obtained from Table 1-4.

The vertical pseudoskin factor s_V can be calculated after certain dimensionless variables are determined:

$$h_D = \frac{h}{l_p} \sqrt{\frac{k_H}{k_V}}, \qquad (1\text{-}55)$$

where h is the distance between perforations and is exactly inversely proportional to the shot density;

$$r_{pD} = \frac{r_{perf}}{2h} \left(1 + \sqrt{\frac{k_V}{k_H}} \right), \qquad (1\text{-}56)$$

where r_{perf} is the perforation radius; and

$$r_{wD} = \frac{r_w}{l_p + r_w}. \qquad (1\text{-}57)$$

The vertical pseudoskin effect is then

$$s_V = 10^a h_D^{b-1} r_{pD}^b, \qquad (1\text{-}58)$$

where a and b are

$$a = a_1 \log r_{pD} + a_2 \qquad (1\text{-}59)$$

$$b = b_1 r_{pD} + b_2. \qquad (1\text{-}60)$$

The values of the constants a_1, a_2, b_1 and b_2 are given in Table 1-5 as functions of the phasing angle θ.

Finally, the wellbore skin effect s_{wb} can be approximated by

$$s_{wb} = c_1 e^{c_2 r_{wD}}. \qquad (1\text{-}61)$$

The constants c_1 and c_2 can be obtained from Table 1-6.

As an example, assume $r_w = 0.406$ ft, $l_p = 0.667$ ft, $h = 0.333$ ft (3 shots per foot [spf]), $k_H/k_v = 3$, $r_{perf} = 0.0208$ ft [0.25 in.] and $\theta = 90°$.

From Eq. 1-54 and Table 1-4, $r_w'(\theta) = 0.779$ ft, and thus from Eq. 1-53, $s_H = -0.65$. From Eqs. 1-55, 1-56 and 1-57, the dimensionless variables h_D, r_{pD} and r_{wD} are equal to 0.86, 0.05 and 0.38, respectively. From Eq. 1-59 and Table 1-5, $a = 2.58$, and from Eq. 1-60 and Table 1-5, $b = 1.73$. Then, from

Table 1-3. Pseudoskin factors for partially penetrating slanted wells (Cinco-Ley et al., 1975).

θ_w (°)	z_{wD}/h_D	$\dfrac{h_{wD}\cos\theta_w}{h_D}$	$s_{\theta+c}$	s_c	s_θ	θ_w (°)	z_{wD}/h_D	$\dfrac{h_{wD}\cos\theta_w}{h_D}$	$s_{\theta+c}$	s_c	s_θ
			$h_D = 100$						**$h_D = 100$ continued**		
0	0.95	0.1	20.810	20.810	0	0	0.6	0.5	2.430	2.430	0
15			20.385	20.810	−0.425	15			2.254	2.430	−0.176
30			18.948	20.810	−1.861	30			1.730	2.430	−0.700
45			16.510	20.810	−4.299	45			0.838	2.430	−1.592
60			12.662	20.810	−8.147	60			−0.466	2.430	−2.897
75			6.735	20.810	−14.074	75			−2.341	2.430	−4.772
0	0.8	0.1	15.809	15.809	0	0	0.5	0.5	2.369	2.369	0
15			15.449	15.809	−0.36	15			2.149	2.369	−0.175
30			14.185	15.809	−1.623	30			1.672	2.369	−0.697
45			12.127	15.809	−3.682	45			0.785	2.369	−1.584
60			8.944	15.809	−6.864	60			−0.509	2.369	−2.879
75			4.214	15.809	−11.594	75			−2.368	2.369	−4.738
0	0.6	0.1	15.257	15.257	0	0	0.625	0.75	0.924	0.924	0
15			14.898	15.257	−0.359	15			0.778	0.924	−0.145
30			13.636	15.257	−1.621	30			0.337	0.924	−0.587
45			11.583	15.257	−3.674	45			−0.411	0.924	−1.336
60			8.415	15.257	−6.842	60			−1.507	0.924	−2.432
75			3.739	15.257	−11.517	75			−3.099	0.924	−4.024
0	0.5	0.1	15.213	15.213	0	0	0.5	0.75	0.694	0.694	0
15			14.854	15.213	−0.359	15			0.554	0.694	−0.139
30			13.592	15.213	−1.620	30			0.134	0.694	−0.560
45			11.540	15.213	−3.673	45			−0.581	0.694	−1.275
60			8.372	15.213	−6.841	60			−1.632	0.694	−2.326
75			3.699	15.213	−11.514	75			−3.170	0.694	−3.864
0	0.875	0.25	8.641	8.641	0	0	0.5	1	0	0	0
15			8.359	8.641	−0.282	15			−0.128	0	−0.128
30			7.487	8.641	−1.154	30			−0.517	0	−0.517
45			5.968	8.641	−2.673	45			−1.178	0	−1.178
60			3.717	8.641	−4.924	60			−2.149	0	−2.149
75			0.464	8.641	−8.177	75			−3.577	0	−3.577
0	0.75	0.25	7.002	7.002	0				**$h_D = 1000$**		
15			6.750	7.002	−0.251	0	0.95	0.1	41.521	41.521	0
30			5.969	7.002	−1.032	15			40.343	41.521	−1.178
45			4.613	7.002	−2.388	30			36.798	41.521	−4.722
60			2.629	7.002	−4.372	45			30.844	41.521	−10.677
75			−0.203	7.002	−7.206	60			22.334	41.521	−19.187
						75			10.755	41.521	−30.766
0	0.6	0.25	6.658	6.658	0	0	0.8	0.1	35.840	35.840	0
15			6.403	6.658	−0.249	15			34.744	35.840	−1.095
30			5.633	6.658	−1.024	30			31.457	35.840	−4.382
45			4.290	6.658	−2.447	45			25.973	35.840	−9.867
60			2.337	6.658	−4.32	60			18.241	35.840	−17.599
75			−0.418	6.658	−7.076	75			8.003	35.840	−27.837
0	0.5	0.25	6.611	6.611	0	0	0.6	0.1	35.290	35.290	0
15			6.361	6.611	−0.249	15			34.195	35.290	−1.095
30			5.587	6.611	−1.023	30			30.910	35.290	−4.380
45			4.245	6.611	−2.365	45			25.430	35.290	−9.860
60			2.295	6.611	−4.315	60			17.710	35.290	−17.580
75			−0.451	6.611	−7.062	75			7.522	35.290	−27.768
0	0.75	0.5	3.067	3.067	0	0	0.5	0.1	35.246	35.246	0
15			2.878	3.067	−0.189	15			34.151	35.246	−1.095
30			2.308	3.067	−0.759	30			30.866	35.246	−4.380
45			1.338	3.067	−1.729	45			25.386	35.246	−9.860
60			−0.082	3.067	−3.150	60			17.667	35.246	−17.579
75			−2.119	3.067	−5.187	75			7.481	35.246	−27.765

Table 1-3. Pseudoskin factors for partially penetrating slanted wells (Cinco-Ley *et al.*, 1975) *continued.*											
θ_w (°)	z_{wD}/h_D	$\dfrac{h_{wD}\cos\theta_w}{h_D}$	$s_{\theta+c}$	s_c	s_θ	θ_w (°)	z_{wD}/h_D	$\dfrac{h_{wD}\cos\theta_w}{h_D}$	$s_{\theta+c}$	s_c	s_θ
$h_D = 1000$ *continued*						$h_D = 1000$ *continued*					
0	0.875	0.25	15.733	15.733	0	0	0.6	0.5	4.837	4.837	0
15			15.136	15.733	−0.597	15			4.502	4.837	−0.335
30			13.344	15.733	−2.389	30			3.503	4.837	−1.334
45			10.366	15.733	−5.367	45			1.858	4.837	−2.979
60			6.183	15.733	−9.550	60			−0.424	4.837	−5.261
75			0.632	15.733	−15.101	75			−3.431	4.837	−8.268
0	0.75	0.25	14.040	14.040	0	0	0.5	0.5	4.777	4.777	0
15			13.471	14.040	−0.569	15			4.443	4.777	−0.334
30			11.770	14.040	−2.270	30			3.446	4.777	−1.331
45			8.959	14.040	−5.081	45			1.806	4.777	−2.971
60			5.047	14.040	−8.993	60			−0.467	4.777	−5.244
75			−0.069	14.040	−14.109	75			−3.458	4.777	−8.235
0	0.6	0.25	13.701	13.701	0	0	0.625	0.75	1.735	1.735	0
15			13.133	13.701	−0.568	15			1.483	1.735	−0.252
30			11.437	13.701	−2.264	30			0.731	1.735	−1.004
45			8.638	13.701	−5.063	45			−0.512	1.735	−2.247
60			4.753	13.701	−8.948	60			−2.253	1.735	−3.988
75			−0.288	13.701	−13.989	75			−4.595	1.735	−6.330
0	0.5	0.25	13.655	13.655	0	0	0.5	0.75	1.508	1.508	0
15			13.087	13.655	−0.568	15			1.262	1.508	−0.246
30			11.391	13.655	−2.264	30			0.528	1.508	−0.980
45			8.593	13.655	−5.062	45			−0.683	1.508	−2.191
60			4.711	13.655	−8.944	60			−2.380	1.508	−3.888|
75			−0.321	13.655	−13.976	75			−4.665	1.508	−6.173
0	0.75	0.5	5.467	5.467	0	0	0.5	1	0	0	0
15			5.119	5.467	−0.348	15			−0.206	0	−0.206|
30			4.080	5.467	−1.387	30			−0.824	0	−0.824
45			2.363	5.467	−3.104	45			−1.850	0	−1.850
60			−0.031	5.467	−5.498	60			−3.298	0	−3.298
5			−3.203	5.467	−8.670	75			−5.282	0	−5.282

Table 1-4. Dependence of α_θ on phasing.	
Perforating Phasing (°)	α_θ
0 (360)	0.250
180	0.500
120	0.648
90	0.726
60	0.813
45	0.860

Table 1-5. Vertical skin correlation coefficients.				
Perforating Phasing (°)	a_1	a_2	b_1	b_2
0 (360)	−2.091	0.0453	5.1313	1.8672
180	−2.025	0.0943	3.0373	1.8115
120	−2.018	0.0634	1.6136	1.7770
90	−1.905	0.1038	1.5674	1.6935
60	−1.898	0.1023	1.3654	1.6490
45	−1.788	0.2398	1.1915	1.6392

Eq. 1-58, $s_V = 1.9$, and from Eq. 1-61 and Table 1-6, $s_{wb} = 0.02$.

The total perforation skin effect obtained with Eq. 1-52 is equal to 1.3 for this example.

- Combination of damage and perforation skin effect

  Karakas and Tariq (1988) showed that the damage and perforation skin effect can be approximated by

$$(s_d)_p = \left(\frac{k}{k_s}-1\right)\left[\ln\frac{r_s}{r_w}+s_p\right] = (s_d)_o + \frac{k}{k_s}s_p,$$

(1-62)

where the perforations terminate inside the damage zone ($l_p < l_d$), r_s is the damage zone radius, and $(s_d)_o$ is the equivalent openhole skin effect

Table 1-6. Variables c_1 and c_2.		
Perforating Phasing (°)	c_1	c_2
0 (360)	1.6E–1	2.675
180	2.6E–2	4.532
120	6.6E–3	5.320
90	1.9E–3	6.155
60	3.0E–4	7.509
45	4.6E–5	8.791

(Eq. 1-45). If, for example, $l_p = 1.2$ ft ($r_s = 1.606$ ft) and the permeability reduction ratio $k/k_s = 5$, from Eq. 1-62 and the perforation skin effect calculated in the previous section, $(s_d)_p = 12$.

Karakas and Tariq (1988) also showed that the damage skin effect for perforations terminating outside the damaged zone can be approximated by

$$\left(s_d\right)_p = s_p - s_p', \qquad (1\text{-}63)$$

where s_p' is the perforation skin effect evaluated at the modified perforation length l_p' and modified radius r_w':

$$l_p' = l_p - \left(1 - \frac{k_s}{k}\right)l_d \qquad (1\text{-}64)$$

$$r_w' = r_w + \left(1 - \frac{k_s}{k}\right)l_d. \qquad (1\text{-}65)$$

The quantities l_p' and r_w' are used instead of l_p and r_w, respectively, to calculate s_p as presented in Section 1-3.4.

Assume that in the previous example $l_d = 0.4$ ft, which makes the modified length l_p' and modified radius r_w' equal to 0.347 and 0.726 ft, respectively. From Eq. 1-63, $(s_d)_p = 1$, which is a marked decrease from the value calculated for the length of the damage larger than the length of the perforations.

1-3.5. Hydraulic fracturing in production engineering

If removal of the skin effect by matrix stimulation and good completion practices does not lead to an economically attractive well, the potential benefit

from hydraulic fracturing is illustrated by revisiting "Example of steady-state IPR: skin effect variation" (page 1-4). With permeability equal to 5 md, the reduction in the skin effect from 10 to 0 (e.g., $p_{wf} = 2000$ psi) results in production rates of 560 and 1230 STB/D, respectively, and this difference of 670 STB/D is clearly an attractive target for matrix stimulation. However, at a permeability of 0.05 md, all rates would be divided by 100, resulting in an incremental production of only 6.7 STB/D.

Interestingly, for $k = 0.05$ md, reducing the skin effect to –5 leads to a poststimulation production rate equal to 30 STB/D and an incremental production rate (over the $s = 10$ case and $k = 0.05$ md) of about 25 STB/D. Such an equivalent skin effect can be the result of hydraulic fracturing.

A great portion of this volume is devoted to this type of stimulation, its fundamental background and the manner with which it is applied in petroleum engineering. Here, hydraulic fractures are presented as well production or injection enhancers.

Prats (1961), in a widely cited publication, presented hydraulic fractures as causing an effective wellbore radius and, thus, an equivalent skin effect once the well enters (pseudo)radial flow. In other words, the reservoir flows into a fractured well as if the latter has an enlarged wellbore. Figure 1-10 is Prats' development graphed as the dimensionless effective wellbore radius r_{wD}' versus the relative capacity parameter a.

The dimensionless relative capacity parameter has been defined as

$$a = \frac{\pi k x_f}{2 k_f w}, \qquad (1\text{-}66)$$

where k is the reservoir permeability, x_f is the fracture half-length, k_f is the fracture permeability, and w is the fracture width.

The dimensionless effective wellbore radius is simply

$$r_{wD}' = \frac{r_w'}{x_f} = \frac{r_w e^{-s_f}}{x_f}. \qquad (1\text{-}67)$$

Thus, if x_f and $k_f w$ are known (as shown later in this volume, this is the essence of hydraulic fracturing), then Fig. 1-10 enables calculation of the equivalent skin effect s_f that the well will appear to have while it flows under pseudoradial conditions. Cinco-
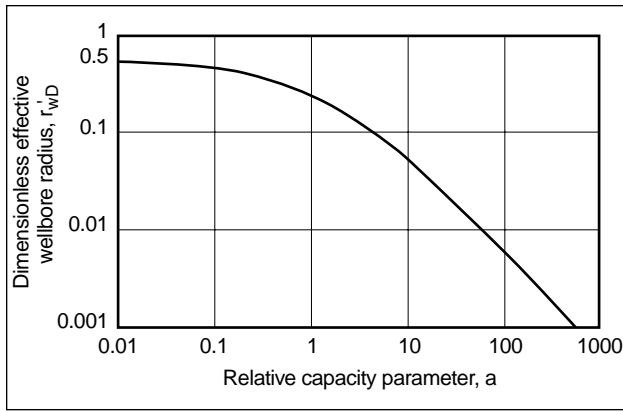
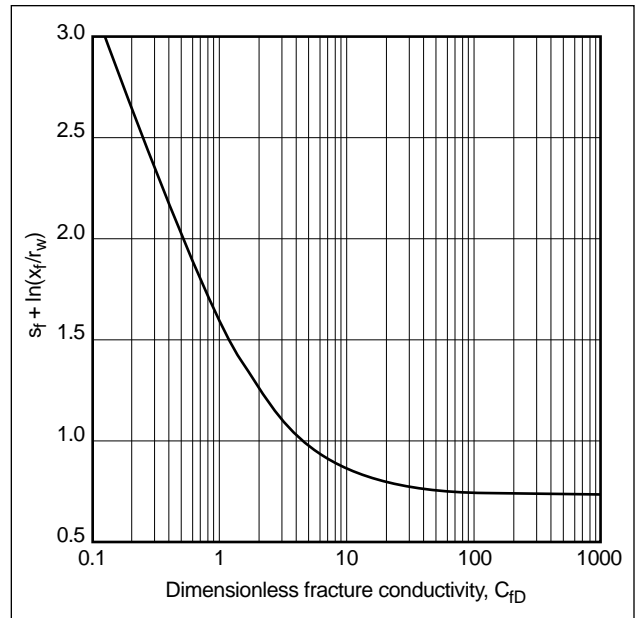**Figure 1-10.** *Dimensionless effective wellbore radius of a hydraulically fractured well (Prats, 1961).*

Ley and Samaniego-V. (1981b) later introduced a direct correlation for s_f (Fig. 1-11).

Graphed on the x-axis of Fig. 1-11 is the dimensionless fracture conductivity C_{fD}, which is simply

$$C_{fD} = \frac{k_f w}{k_f x} \qquad (1\text{-}68)$$

and is related to Prats' relative capacity by

$$C_{fD} = \frac{\pi}{2a}. \qquad (1\text{-}69)$$

The following example illustrates the impact of a hydraulic fracture on well production.

• Example calculation of production from a hydraulically fractured well

Using the variables in "Example of steady-state IPR: skin effect variation" (page 1-4) but with $k = 0.5$ md, demonstrate the production improvement from a hydraulic fracture at $C_{fD} = 5$ and $x_f = 500$ ft. Also, compare this result with the pretreatment production if $s = 10$ and after a matrix stimulation, assuming that all skin effect is eliminated ($s = 0$). Use $p_{wf} = 2000$ psi.

Solution

The IPR for this well is simply

$$q = 0.345 \left(\frac{5000 - p_{wf}}{8.43 + s} \right).$$

Using Fig. 1-11 (Fig. 1-10 can also be used) and $C_{fD} = 5$:

Figure 1-11. *Equivalent fracture skin effect (Cinco-Ley and Samaniego-V., 1981b).*

$$s_f + \ln \frac{x_f}{r_w} = 0.9,$$

which for $x_f = 500$ ft and $r_w = 0.328$ ft gives $s_f = -6.4$.

The production rates at pretreatment ($s = 10$), after matrix stimulation ($s = 0$) and after fracturing ($s = -6.4$) are 56, 123 and 518 STB/D, respectively.

• General requirements for hydraulic fractures

What general requirements should be expected from the design of hydraulic fractures? As discussed in later chapters of this volume, the execution of a hydraulic fracture should provide a fracture length and propped width, and selection of the proppant and fracturing fluid is crucial for fracture permeability. Because of physical constraints the resulting values may not be exactly the desired ideal values, but certain general guidelines should permeate the design.

The dimensionless fracture conductivity C_{fD} is a measure of the relative ease with which the reservoir (or injected) fluid flows among the well, fracture and reservoir. Obviously, in a low-permeability reservoir even a fracture of narrow width and relatively low permeability results de facto in a high-conductivity fracture. The limiting value is an infinite-conductivity fracture, which mathemati-

cally implies that once fluid enters the fracture it is instantaneously transported into the well. Thus, in low-permeability reservoirs, the length of the fracture is critical and the design must consider this requirement. The longer the fracture, subject to the economic constraints of its execution, the more desirable it is.

Conversely, for high-permeability reservoirs, as shown by Eq. 1-68, to increase C_{fD} requires increasing the $k_f w$ product. Thus, maximizing conductivity must be the major result from the design. Arresting the length growth and inflating the fracture are means to accomplish this purpose. A process involving tip screenout (TSO) has been developed, exactly to effect such a fracture geometry.

- Optimal fracture conductivity

  With advent of the TSO technique especially in high-permeability, soft formations (called frac and pack), it is possible to create short fractures with unusually wide propped widths. In this context a strictly technical optimization problem can be formulated: how to select the length and width if the propped fracture volume is given. The following example from Valkó and Economides (1995) addresses this problem, using the method derived by Prats (1961).

- Example of optimal fracture conductivity

  Consider the following reservoir and well data: $k = 0.4$ md, $h = 65$ ft, $r_e/r_w = 1000$, $\mu = 1$ cp, $p_e = 5000$ psi and $p_{wf} = 3000$ psi. Determine the optimal fracture half-length x_f, optimal propped width w and optimal steady-state production rate if the volume of the propped fracture is $V_f = 3500$ ft^3. Use a value of 10,000 md for the fracture permeability k_f, taking into account possible damage to the proppant, and assume that the created fracture height equals the formation thickness. Use the Cinco-Ley and Samaniego-V. (1981b) graph (Fig. 1-11), which assumes pseudoradial flow.

  Solution

  The same propped volume can be established by creating a narrow, elongated fracture or a wide but short one. In all cases the production rate can be obtained from Eq. 1-9, which with the incorporation of s_f takes the form

$$q = \frac{kh\Delta p}{141.2 B\mu \left(\ln \dfrac{r_e}{r_w} + s_f \right)} .$$

Obviously, the aim is to minimize the denominator.

This optimization problem was solved by Prats (1961) for steady-state flow. He found the maximum production rate occurs at $a = 1.25$ ($C_{fD} = 1.26$ from Eq. 1-69). For this value of a, $r_w'/x_f = 0.22$ from Fig. 1-10 and Eq. 1-66 gives

$$x_f / w = 0.8 k_f / k = 0.8 \times 10,000 / 0.4 = 20,000 .$$

Using $V_f = 2whx_f$ with this x_f/w ratio,

$$x_f^2 = 20,000 V_f / 2h = (20,000 \times 3500)/(2 \times 65),$$

and $x_f = 730$ ft; hence, $w = x_f /2000 = 0.037$ ft $= 0.44$ in. From $r_w' = 0.22 \, x_f$ and $r_w = 0.33$ ft, Eq. 1-7 gives $r_w'/r_w = e^{-s} = 490$, and $s = -(\ln 490) = -6.1$.

For $p_e = 5000$ psi and $p_{wf} = 3000$ psi, the optimized production rate is

$$q = \frac{(0.4)(65)(2000)}{(141.2)(1)(1)(\ln 3000 - 6.2)} = 204 \text{ STB} / \text{D} .$$

It is necessary to check if the resulting half-length is less than r_e (otherwise x_f must be selected to be equal to r_e). Similarly, the resulting optimal width must be realistic; e.g., it is greater than 3 times the proppant diameter (otherwise a threshold value must be selected as the optimal width). In this example both conditions are satisfied.

This example provides an insight into the real meaning of dimensionless fracture conductivity. The reservoir and the fracture can be considered a system working in series. The reservoir can deliver more hydrocarbons if the fracture is longer, but with a narrow fracture, the resistance to flow may be significant inside the fracture itself. The optimal dimensionless fracture conductivity $C_{fD,opt} = 1.26$ in this example corresponds to the best compromise between the requirements of the two subsystems.

1-4. Tubing performance and NODAL* analysis

The inflow performance relationships described in Section 1-2 provide a picture of the pressure and rates that a reservoir with certain characteristics (permeability, thickness, etc.), operating under certain

conditions (pressure, mode of flow), can deliver into the bottomhole of a well. The fluid must traverse a path from the bottom of the well to the top and then into surface equipment such as a separator. Figure 1-12 describes such a path, which consists of several segments, joints and valves, all of which cause a pressure drop. NODAL analysis considers the reservoir/wellbore system and uses calculations of the pressure loss across each segment to predict the production rate and identify any restrictions that may reduce the hydrocarbon flow rate.

At its simplest manifestation, for a given wellhead pressure, tubing performance allows calculation of the required bottomhole flowing pressure to lift a range of flow rates to the top. The total pressure drop in the well consists of the hydrostatic and friction pressure drops.

Several correlations for tubing performance are in use in the petroleum industry (Beggs and Brill, 1973; Hagedorn and Brown, 1965). Brown (1977), in a widely used work, outlined the procedure for pressure drop calculations in production strings as shown

in Fig. 1-13 for two wellhead flowing pressures. As the flow rate increases (on the right side of the curves) the required bottomhole flowing pressure increases, reflecting higher friction pressures at the higher rates. On the left side of the curves, the peculiar shape is due to liquid holdup; lower rates do not have sufficient momentum to purge liquid accumulation in the well, resulting in an unavoidable increase in the hydrostatic pressure.

The correlations to calculate the required pressure drops take full account of the phase behavior of the, almost always, two-phase oil and gas mixture. An increase in the wellhead pressure ordinarily results in a disproportionate increase in the bottomhole pressure because the higher pressure level in the tubing causes a more liquid-like fluid and a larger hydrostatic pressure component (density is higher).

Combining the tubing performance curve, often known in vertical wells as the vertical lift performance (VLP), with an IPR provides the well deliverability at the determined bottomhole flowing pressure (Fig. 1-14).
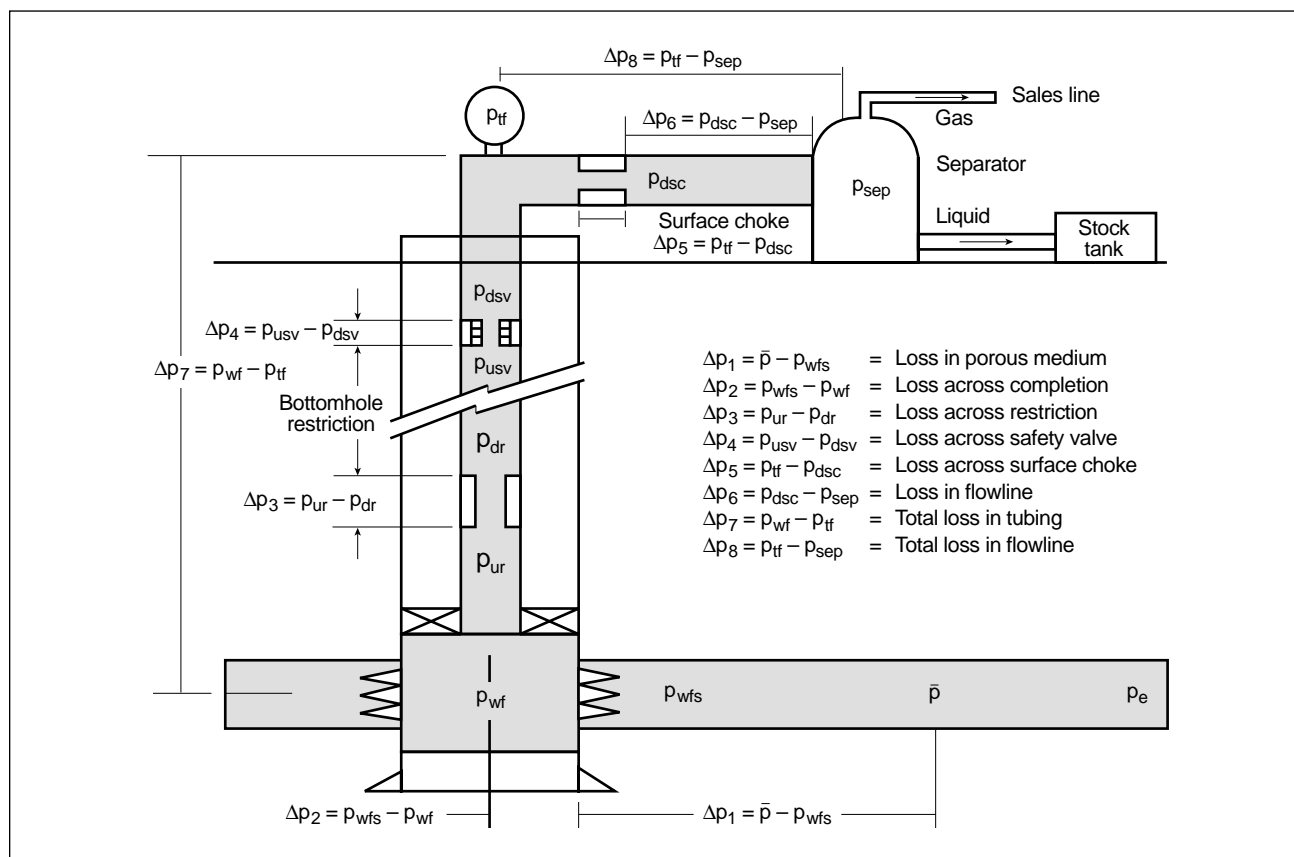

Figure 1-12. *Well hydraulic system.* p_{dr} = *downstream restriction pressure,* p_{dsc} = *pressure downstream of the surface choke,* p_{dsv} = *pressure downstream of the safety valve,* p_{sep} = *separator pressure,* p_{tf} = *tubing flowing pressure,* p_{ur} = *upstream restriction pressure,* p_{usv} = *pressure upstream of the safety valve,* p_{wfs} = *wellbore sandface pressure.*
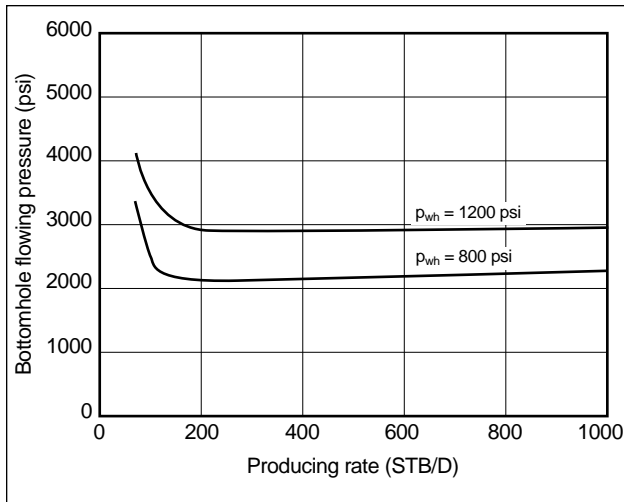
Figure 1-13. *Vertical lift performance (also known as tubing intake) curves for two values of wellhead flowing pressure* p_{wh}.

Figure 1-14. *IPR and VLP curves combined for the prediction of well deliverability.*
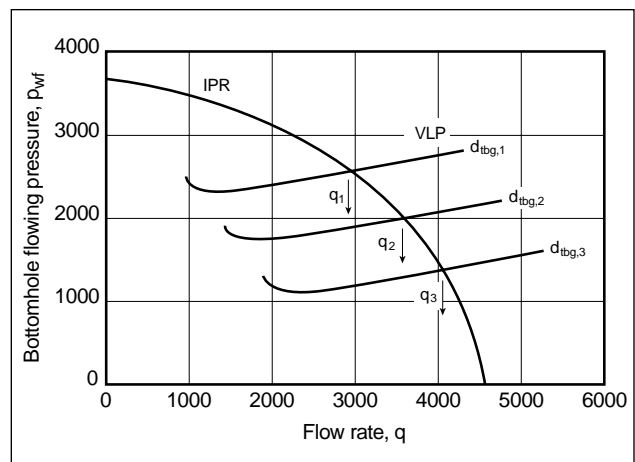
Figure 1-15. *VLP curve variation for different tubing diameters (*d_{tbg}*) and the effect on well deliverability.*

NODAL analysis is one of the most powerful tools in production engineering. It can be used as an aid in both the design and optimization of well hydraulics and IPR modification. Figure 1-15 shows one of the most common uses of NODAL analysis. The well IPR is plotted with three VLP curves (e.g., each corresponding to a different wellhead pressure—and perhaps a different artificial lift mechanism—in the case of an oil well or a different tubing diameter in a gas well). The three different production rates over time can be balanced against the incremental economics of the various well completion options.

Figure 1-16 demonstrates a single VLP but three different IPRs (e.g., each corresponding to a different hydraulic fracture design). Again, the incremental benefits over time must be balanced against the incremental costs of the various fracture designs.

The use of NODAL analysis as an engineering investigative tool is shown in Fig. 1-17. Suppose that several perforations are suspected of being closed. A calculation allowing several different scenarios of the number of open perforations and comparison with the actual flow rate can provide a convincing answer to the problem.

1-5. Decision process for well stimulation

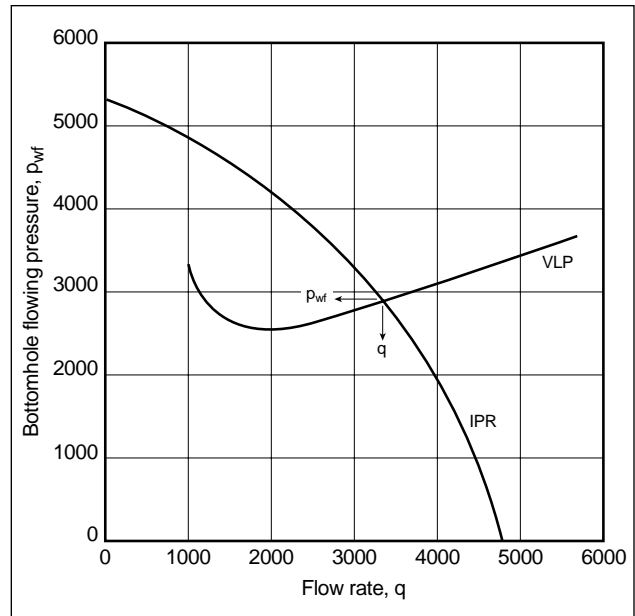To be done properly, the engineering exercise of the decision process for well stimulation requires considerable knowledge of many diverse processes. Few activities in the petroleum or related industries use such a wide spectrum of sciences and technologies as well stimulation, both matrix and fracturing. This volume is intended to present these technologies and their interconnections.

As with many engineering processes, stimulation must culminate in the design, selection of the specific treatment and, of course, selection of candidate wells. To choose among the various options, of which one is to do nothing, a means for an economic comparison of the incremental benefits weighted against the costs is necessary.
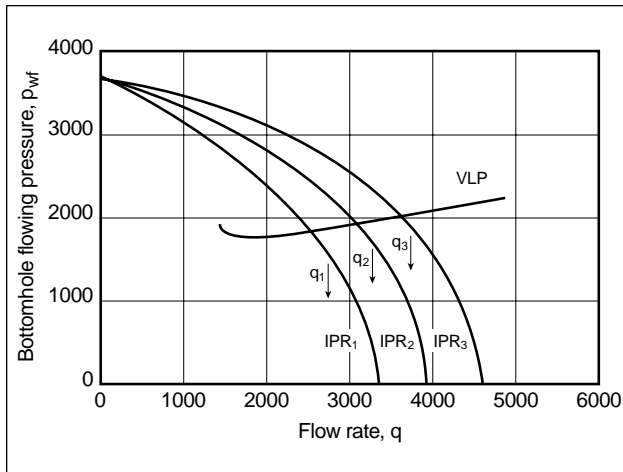
Figure 1-16. *IPR curve variation (e.g., for different skins) and the effect on well deliverability.*

Figure 1-17. *Well diagnosis (e.g., for unknown number of open perforations N_{perf}) using a comparison of predicted versus actual IPRs.*

1-5.1. Stimulation economics

Because the whole purpose of stimulation is to increase the value of the producing property through an accelerated production rate or increased recovery, economics should be the driver in deciding whether to conduct the stimulation, what type of stimulation to do and which various aspects of the treatment to include.

Several economic indicators can be used to show the value of stimulation. Because of the wide variety of operating conditions, companies may not have a single indicator for the "answer" in all stimulation investments. Although the common ground in economics is profit, in many petroleum activities liquidity, risk and corporate goals may make it necessary to choose investments that differ from the ultimate maximum value of a project.

The oldest indicator used in oil production is payout time, which is the amount of time necessary to recoup the money invested. If the actual time is less than the required time, the investment is considered attractive:

$$\sum_{n=1}^{n} \Delta\$_n - cost = 0, \qquad (1\text{-}70)$$

where $\Delta\$_n$ is the incremental revenue (minus the incremental expenses and taxes that are due to operations), n is the time period increments (e.g., years) in which it is received, and *cost* consists of the total expenses associated with the stimulation. This indicator does not provide for the time value of money
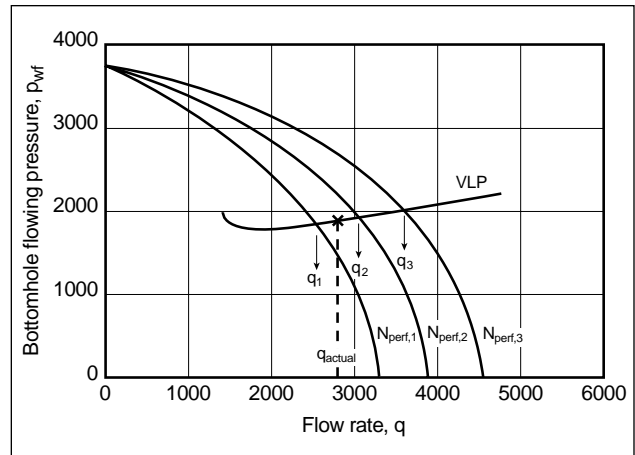
or the net value (profit) for the operator; rather, it is a measure of liquidity or how fast the investment will be recovered.

The indicator can be adjusted to show the time value of money (discounted payout), the hurdle rate necessary for the company to invest or both factors. The hurdle rate is the annualized percentage of return that must be achieved to make the project as good an investment as the average company investment. The discounted payout is

$$\sum_{n=1}^{n} \frac{\Delta\$_n}{(1+i)^n} - cost = 0. \qquad (1\text{-}71)$$

The interest (hurdle) rate i is the indicator that suggests when the investment will be returned without lowering the corporate investment returns and accounting for inflation (time value of money).

When the full stream of cash flows for the projected relative life of the project is used, an indicator called net present value (NPV) is defined as

$$NPV = \sum_{n=1}^{n} \frac{\Delta\$_n}{(1+i)^n} - cost. \qquad (1\text{-}72)$$

NPV gives a dollar value added to the property at present time. If it is positive, the investment is attractive; if it is negative, it means an undesirable investment. NPV is the most widely used indicator showing a dollar amount of net return.

To get an indicator on relative profitability against more global investments such as stocks, bonds and corporate profits, the rate of return (ROR) is used.

ROR is simply varying i to get an NPV equal to zero. That value of i is the ROR. The limitation in using the ROR indicator is that it does not provide a mechanism of how the cash comes in (cash flow versus time).

In Fig. 1-18 there are two investment possibilities. A has the highest NPV for small interest rates but falls off quickly with increasing rates, whereas B has a smaller NPV with low rates but remains flatter as rates rise. This means that A makes more money, but as interest rates rise its return is hurt more than that for B. B pays the money back with a better ROR, even if it has a smaller NPV at low interest rates.

Another indicator of investment profitability is the benefits to cost ratio (BCR):

$$BCR = \frac{NPV}{cost}, \qquad (1\text{-}73)$$

which shows the relationship of relative return for a given investment (cost) size. BCR is a good indicator if there are more investment opportunities than money to invest.
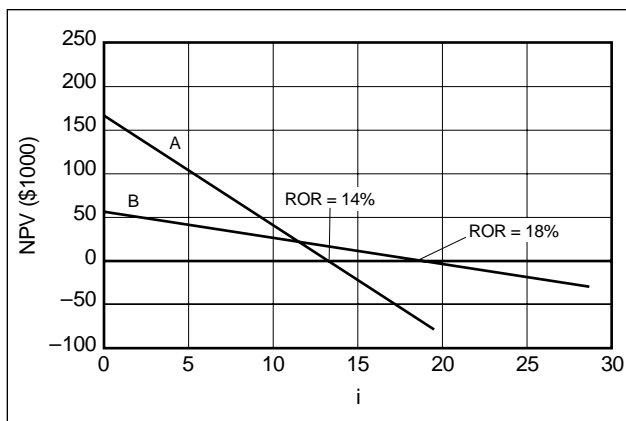

Figure 1-18. *Determination of the rate of return for projects A and B.*

1-5.2. Physical limits to stimulation treatments

Physical limits are dominant aspects for stimulation treatment decisions as often as economic indicators. For the well, these include the following:

- Maximum allowable treating pressure limits injection rates and the type of treating fluids.
- Tubular size limits rates and pipe erosion.

- Well location size limits the equipment and materials that can be used.
- Tubular integrity prevents or limits the type of treatments that can be employed without compromise.
- Completion tools and their location limit where the treatment is placed and the magnitude of the rates and volumes.
- Zonal isolation is whether the zone can be isolated from other intervals through perforating and/or pipe integrity limitations.

  Typical reservoir constraints are

- production failures: water or gas coning or influx, formation sanding
- physical location of the zones and their thicknesses: pay zone qualities limit or dictate treatments.

1-6. Reservoir engineering considerations for optimal production enhancement strategies[†]

Cost-effective production improvement has been the industry focus for the past several years. Fracturing, stimulating, reperforating and recompleting existing wells are all widely used methods with proven results in increasing the NPV of old fields. Now reentry drilling is generating high interest for the potential it offers to improve recovery from damaged or depleted zones or to tap into new zones at a generally low cost. Applied to mature reservoirs, all these strategies have the advantage of starting with a fair to good reservoir description as well as a working trajectory to the target formation. Even when a new well is drilled, the decision whether to drill a vertical, slanted or horizontal well and how to complete the productive interval can profoundly effect the well's productivity and the size of the volume drained by the well. Today's technology also entertains multiple branches from a main trunk, which may be a newly drilled or existing well.

1-6.1. Geometry of the well drainage volume

The geometry of the well drainage volume depends on the well trajectory within the productive zone, neighboring wells, geometry of hydraulic fractures, nearby reservoir limits and reservoir flow characteristics. Areas drained by an isolated well in an effectively infinite reservoir are diagrammed in Figs. 1-19a and 1-19b. A vertical well creates a circular cylinder pressure sink whereas a hydraulically fractured well creates a pressure sink in the shape of a finite slab with dimensions defined by the formation thickness and the total fracture length. With adequate vertical permeability the horizontal well drainage area is similar to that of a vertical fracture, with the total fracture length equal to that of the horizontal well. The extent of the effective drainage area is approximately defined by the locus of points equidistant from the surface of the pressure sink associated with the well. This forms a circle for a vertical well; an approximate ellipse is formed for hydraulically fractured and horizontal wells.

Wells drilled in a square pattern impose a square drainage area. For vertical wells, this is similar to the circular effective drainage shape (Fig. 1-19c), but for horizontal wells, the equivalent drainage efficiency corresponds to an elongated area. As a rule of thumb, the length of the horizontal well drainage area can be as long as the length of the horizontal well plus one diameter of the comparable vertical well drainage area. For the case in Fig. 1-19d, one-half as many horizontal wells of the length shown could be used to drain the same pattern, as shown in Fig. 1-20a. With longer horizontal wells, even fewer are required.

Figure 1-20b shows another consideration. If the vertical well pattern does not take the direction of maximum horizontal stress $\sigma_{H,max}$ into account,
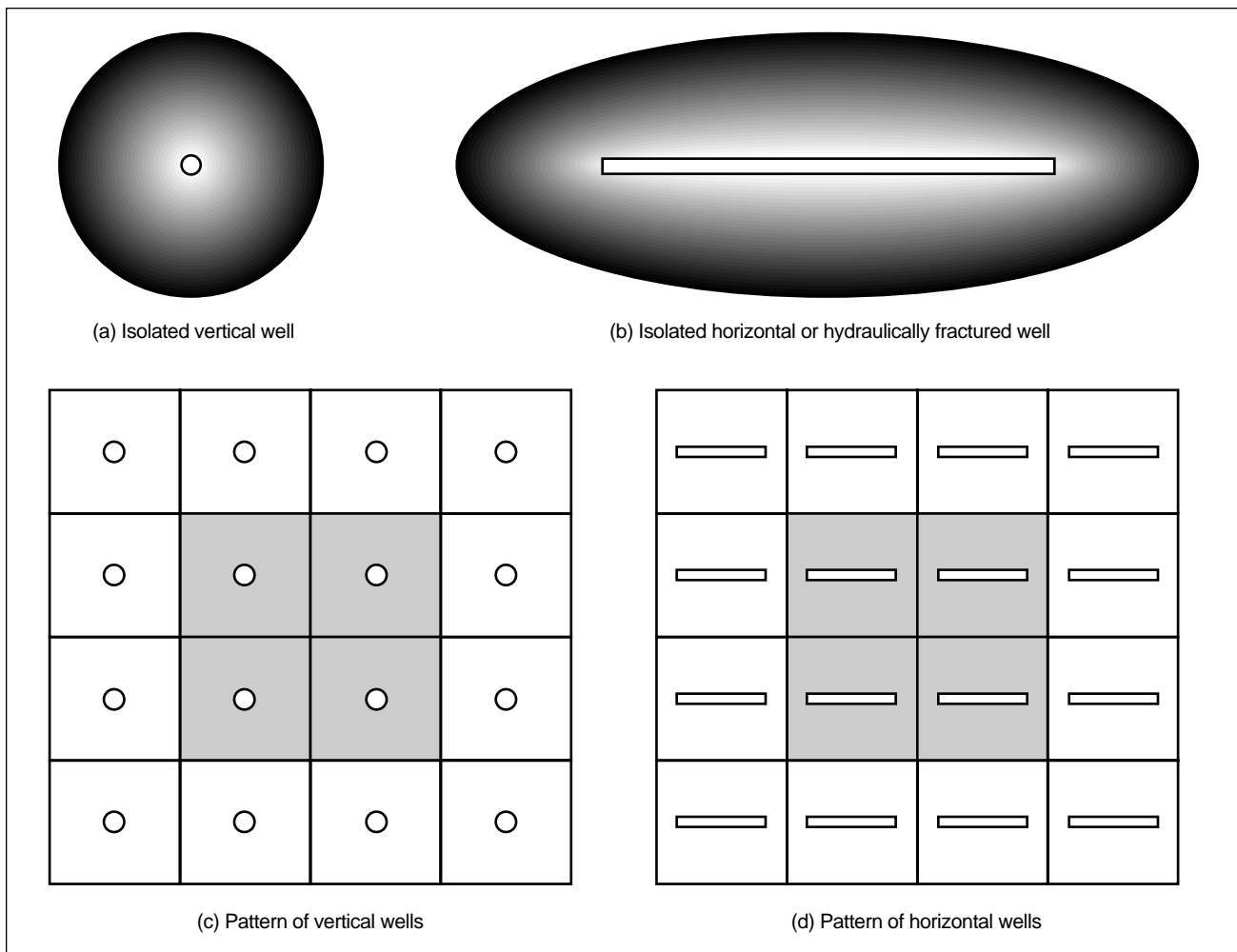

(a) Isolated vertical well

(b) Isolated horizontal or hydraulically fractured well

(c) Pattern of vertical wells

(d) Pattern of horizontal wells

Figure 1-19. *Drainage areas for single and multiple vertical and horizontal wells.*

(a) Pattern of horizontal wells
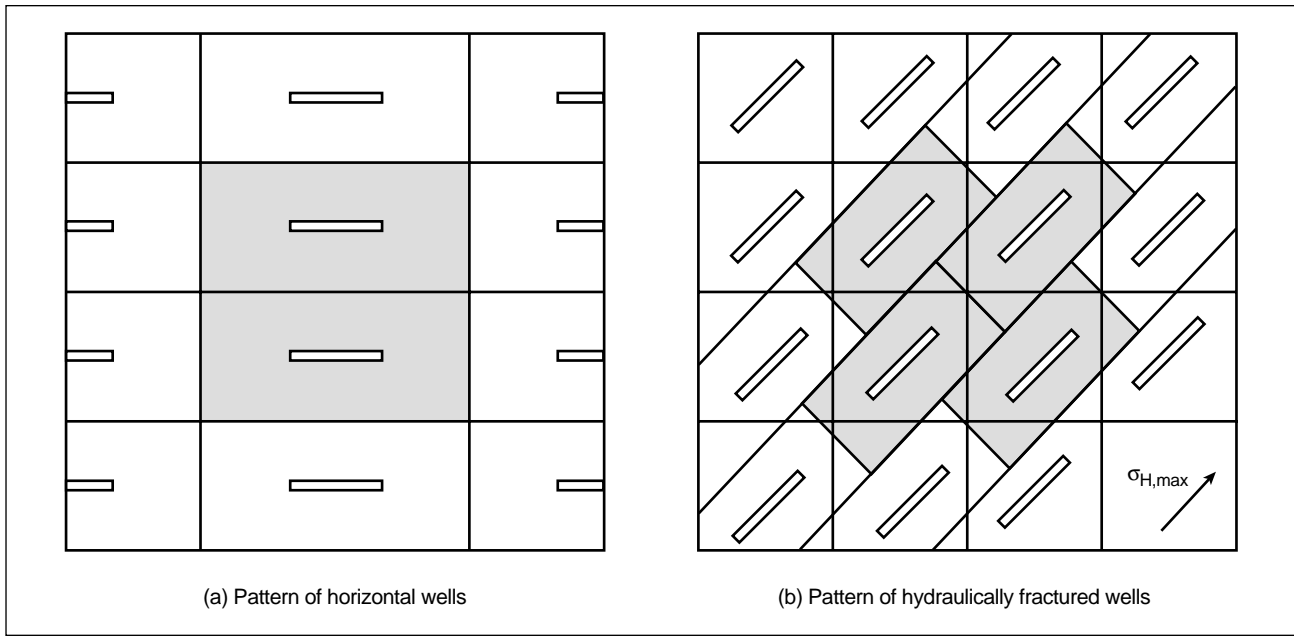
(b) Pattern of hydraulically fractured wells

Figure 1-20. Drainage areas resulting from (a) longer horizontal wells draining more area per well and (b) hydraulically fractured wells in a square pattern that is not in line with the direction of maximum stress.

hydraulically fracturing the wells may result in unplanned drainage geometries.

1-6.2. Well drainage volume characterizations and production optimization strategies

Figures 1-19 and 1-20 assume that the reservoir is homogeneous and isotropic over vast areas. In reality, typical reservoir geology is much more complex. Formation flow characteristics may favor one well geometry over others. The chart in Fig. 1-21 summarizes production optimization strategies for a series of 10 common well drainage volume characterizations. The chart addresses five potential well paths: conventional vertical, hydraulically fractured vertical, slanted, horizontal and hydraulically fractured horizontal. For any one of the drainage volume characterizations, well path options are shown in block diagrams.

Laminated reservoirs (chart row 4 on Fig. 1-21) are a good starting point to understanding the information in the chart. The chart distinguishes layered from laminated by defining a reservoir as layered if the recognized sands are thick enough to be targeted by a horizontal well. If not, the reservoir is classed as laminated. In general, laminated reservoirs have poor vertical permeability. A horizontal well is not

an option in this case because the productivity would be severely penalized by the low vertical permeability, and in a thick formation, a horizontal well may not even produce the entire formation thickness. A vertical well—barefoot, perforated and gravel packed, or gravel packed—can provide excellent productivity in formations with moderate mobility. A slanted well can produce a marginal increase in productivity over a vertical well.

In very high mobility laminated reservoirs (such as turbidites), a frac and pack may provide sand control and the means to bypass near-wellbore damage. However, in a low-mobility reservoir, hydraulically fracturing the well is preferred over any other option because it provides an effective planar sink, greatly increasing the well productivity. For thin and laminated reservoirs, hydraulic fractures in a horizontal well may be the optimal choice because the longer well provides greater reach that increases the drainage volume of the well and the hydraulic fractures enable horizontal flow to the well through the entire formation thickness. Hydraulic fractures in a horizontal well can be planned either as longitudinal, by drilling the well in the direction of maximum horizontal stress, or as transverse, by drilling the well in the direction of minimum stress.

Horizontal wells offer particular advantages in naturally fractured reservoirs (chart row 5 on Fig. 1-21)

Drainage Volume Characterization	Well Path				
	Vertical well	Hydraulically fractured vertical well	Slanted well	Horizontal well	Hydraulically fractured horizontal well
1. Thick and homogeneous, no gas cap or aquifer			$k_V/k_H \geq 0.1$	$k_V/k_H \geq 0.1$	Longitudinal / Transverse
2. Thick and homogeneous, with gas cap and/or aquifer	Gel treatment	Small fracture	Not recommended: risk of premature gas or water production	Closely spaced parallel wells preferred	Not recommended: risk of premature gas or water production
3. Layered			$k_V/k_H \geq 0.1$ preferred over vertical	Stacked parallel wells, with branch flow conformance	
4. Laminated		Hydraulic fracture preferred		Not recommended: risk of disappointing productivity/recovery owing to low vertical permeability	
5. Naturally fractured		Prop natural fractures		Horizontal well to normal to fractures preferred	Reopen natural fractures
6. Naturally fractured under waterflood	Plug fractures connected to injector	Water injection wells	Closely spaced short parallel wells normal to fractures	Water injection wells	Not recommended: risk of premature water breakthrough
7. Structural compartment	Moderate mobility	High mobility / Frac and pack		Drain each with one or more wells	Maximum stress oriented by faults
8. Stratigraphic compartment		High mobility / Frac and pack		Drain each with one or more wells	Hydraulic fracturing may apply in high-mobility cases
9. Elongated compartment		Low mobility	Multiple well paths slanting from single main trunk	Single well traversing multiple channels	Low mobility
10. Attic compartments	Not preferred	Not preferred	Single well traversing multiple beds	One well per bed drilled on strike preferred	Not preferred

Figure 1-21. *Production optimization strategies. Completion options include perforating, gravel packing and stimulation in combination with an applicable strategy.*

when they are drilled normal to the fracture planes. Locating natural fractures and determining their orientation is crucial to developing the best well design in these formations. Hydraulic fracturing places proppant in a series of natural fractures, which typically results in a propped fracture that is parallel to the natural fractures. A horizontal well normal to natural fractures usually provides better productivity than hydraulic fracturing.

Although natural fractures usually are subvertical (nearly vertical), shallower reservoirs and overpressured zones may have subhorizontal (nearly horizontal) fractures open to flow. Vertical and slanted wells are a reasonable choice in these cases. Injection of proppant into horizontal fractures in overpressured zones keeps them open after production lowers the pore pressure. Otherwise, the weight of the overburden tends to close horizontal natural fractures. Likewise, high-pressure injection can reopen natural fractures in depleted zones or natural fractures that were plugged during drilling.

Moving up the chart to the layered reservoirs in row 3 offers an opportunity to address the importance of conformance control. The conventional vertical well commingles production from multiple layers. Productivity and storage capacity contrasts can result in the differential depletion of layers that are not in hydraulic communication vertically other than at the well. In this case, when the production rate is reduced or the well is shut in, crossflow occurs in the wellbore as the higher pressure layers recharge the depleted zones. Another risk of commingled production is that downdip water or updip gas will advance to the well, resulting in early breakthrough of unwanted fluids in the most productive layer or layers. In this case the oil in the lower productivity layers is bypassed. Reentry drilling offers a modern solution by targeting the bypassed oil with a horizontal well.

Strategies for conformance control begin with perforating with a higher shot density in the lower productivity layers. Hydraulic fracturing in layered reservoirs can be useful for conformance control, especially if the treatment is phased to target contrasting zones separately. Unphased, ill-designed hydraulic fracture treatments can be detrimental to production by opening up the high-productivity zones and aggravating the productivity imbalance.

A single horizontal well is not an option for a layered reservoir because it produces from only one layer, but stacked reentry laterals are a highly effective strategy. In the latter design, the length of the lateral can be roughly inversely proportional to the layer's flow capacity. A slanted well offers a less expensive strategy for boosting productivity in a layered reservoir. By designing the trajectory with more drilled length in less productive layers, some conformance control can be achieved. However, if early water breakthrough occurs in the higher productivity layer, it is generally much easier to shut off production in one of the stacked laterals than in a midlength portion of the slanted well.

Hydraulic fracturing in slanted wells is performed typically in offshore wells that commonly follow the same deviation used to reach the reservoir location from a platform. These fractures are typically frac and pack treatments designed for sand control. Because the deviated trajectory may be detrimental to the fracture treatment design, some operators direct the trajectory downward to nearly vertical before passing through the productive formation if hole stability problems do not preclude this approach.

At the top row of the chart in Fig. 1-21 are thick, homogeneous formations. Any of the well path options may be applied for these reservoirs. Mobility extremes may favor hydraulic fracturing, whereas moderate mobility allows using less expensive, conventional vertical well completions. A slanted well may be more cost effective than hydraulic fracturing or a horizontal well, provided that the ratio of vertical to horizontal permeability is not too small. Hydraulic fractures along a horizontal well can compensate for a productivity reduction caused by low vertical permeability in a thick reservoir.

Thick reservoirs with overlying gas or underlying water pose special production problems for which chart row 2 on Fig. 1-21 illustrates some important points. In vertical wells, a strategy to delay bottomwater breakthrough is to perforate near the top of the productive interval. However, the pressure gradient resulting from radial flow toward the well is sufficient to draw the water upward in the shape of a cone. Once the water reaches the deepest perforations, water may be preferentially produced because the water mobility may be greater than oil mobility for low-gravity crudes (owing to the higher oil viscosity) and/or there may be considerable energy to support water production because of a strong bottomwater drive. Once water breakthrough occurs,

there may be little further rise of the cone, and additional oil production will be at an increasing water cut and marginal. One strategy to produce additional oil is to plug back the well above the top of the cone and reperforate. Another is to try to inject gel radially below the perforations. At times, water breakthrough is delayed or avoided with gel injection, and the shape of the cone is widened in any case so that a greater volume of oil is displaced toward the perforations.

A horizontal well drilled near the top of the oil zone above bottomwater produces a pressure gradient normal to the well, and the bottomwater will rise in the shape of a crest instead of a cone. The crest-shaped water advance displaces oil in its path, leading to greater oil recovery than with a vertical well by virtue of the flow geometry. Ehlig-Economides *et al*. (1996) discussed strategies for production enhancement under a strong bottomwater drive. Previous work cited from the literature has analytical estimates for breakthrough time and indicates that recovery efficiency is independent of the production rate under a strong bottomwater drive. Ehlig-Economides *et al.* showed that the relationship between recovery and the spacing of parallel horizontal wells is

$$ r_v = 0.5236 \frac{h}{x_e} \sqrt{k_H/k_V} \left(\frac{3z_w/h - 0.5}{2.5} \right), \qquad (1\text{-}74) $$

that recovery efficiency is a simple function of the half-spacing between wells:

$$ qt_{BT} = \frac{\pi r N}{3} \frac{h}{2x_e} \sqrt{k_H/k_V} \qquad (1\text{-}75) $$

and that the optimal half-spacing between wells is

$$ x_{e,opt} = h\sqrt{k_H/k_V} \, . \qquad (1\text{-}76) $$

In these three equations, r_v is the fraction of the well drainage volume occupied by the crest at the time of water breakthrough. For the optimal well spacing from Eq. 1-76 and a well standoff from the oil-water contact z_w approximately equal to the thickness of the oil column h, the maximum water-free oil recovery (assuming piston-like displacement) is $\pi/6 = 0.5236$. In this case, the optimal interwell spacing is most likely too close for conventional well drilling but may be economical if the laterals can be drilled from a common main trunk.

Interestingly, the same conditions that penalize a horizontal well in a reservoir without overlying gas or underlying water (thick zone, low vertical permeability) favor the horizontal well if overlying gas or underlying water is present. This also illustrates designing the well spacing to be close enough to cause interwell interference. The interwell or inter-lateral interference is beneficial in this case because it both accelerates production and enhances recovery.

Another case that may favor close parallel lateral spacing is in chart row 6 on Fig. 1-21. Although orienting a horizontal well normal to natural fractures boosts well productivity, this approach may risk early water breakthrough, especially in reservoirs under waterflood. Injecting water opposite of a bank of parallel laterals drilled at sufficiently close spacing may allow them to withdraw oil from the matrix rock before the injected water front advances to the production wells. Water may be injected above fracturing pressure to boost injectivity. When horizontal or multilateral wells are not economically justified, the likely short-circuiting of water between vertical well injector/producer pairs may be plugged by gel, thereby forcing the displacement process into the matrix rock.

The remaining rows 7 through 10 on the chart are reminiscent of 3D reservoir geometries. Although conventional vertical wells do not address a 3D reservoir geometry, hydraulically fractured and horizontal wells do, and knowledge of structural and stratigraphic reservoir heterogeneities can greatly improve the design of these wells.

Structural compartmentalization (chart row 7 on Fig. 1-21) results from faults that may not be visible in seismic data interpretations. Even if faults are clearly indicated in the seismic data, only dynamic data derived from formation or well tests or longer term production history matching can establish whether the faults are sealing or conductive. Stratigraphic compartmentalization (chart row 8) is a result of depositional processes. Facies with considerable contrasts in flow characteristics may serve as buffers or flow conduits that act as first-order controls on well productivity and ultimate hydrocarbon recovery. Both structural and stratigraphic heterogeneities may be complicated by diagenetic processes occurring at a later time.

Horizontal wells can target one or more reservoir compartments, and multibranch wells enable shut-off of a branch that produces unwanted gas or water. In

tight reservoirs with considerable faulting, the faults may be associated with natural fractures that can be targeted with horizontal wells, or they may provide reliable information on the maximum stress direction that is essential for planning hydraulic fractures in vertical or horizontal wells.

Stratigraphic limits (chart row 8 on Fig. 1-21) may account for additional reservoir compartmentalization, both vertically and areally. In some cases the reservoir sands may be too thin to be individually identified in a seismic data cross section, but they may have sufficient areal extent to be visible in seismic attribute maps for a structural horizon. In that case, horizontal wells may be an ideal strategy for producing thin formations and for reaching multiple sands.

Chart row 9 on Fig. 1-21 refers to elongated compartmentalization. Although these diagrams depict fluvial reservoir geology, elongated reservoirs can also occur in heavily faulted formations. In either case, the apparent drilling strategies depend on the objective for the well. For example, the well direction can be planned to stay in an elongated reservoir body or to intersect as many reservoir bodies as possible. The latter case implies drilling in the direction normal to the elongation, which for a fluvial reservoir means drilling normal to the downslope direction at the time of deposition. Another approach may be a multibranch well designed to target channels identified with borehole seismic measurements in the horizontal trunk well.

Hydraulic fracturing offers different challenges and possibilities. First, unlike a well trajectory plan, the direction of the hydraulic fracture is not a design choice. Rather, the fracture propagates normal to the direction of minimum stress. A hydraulic fracture may propagate into isolated sand bodies not contacted by the drilled well trajectory, but in other cases the fracture propagation may be inhibited by facies changes or structural discontinuities, and a screenout may occur. In general, drilling solutions may be more flexible in elongated reservoir systems.

The last chart row on Fig. 1-21 is for the special geometry of the attic compartment. In this case, steeply dipping beds may be in contact with an updip gas cap, downdip aquifer or both. One strategy is to drill a horizontal well that passes through several of the beds and stays sufficiently below the updip gas and above the downdip water. Although this seems to be an efficient approach, it suffers from a signifi-

cant disadvantage in that flow is commingled among the layers, and when gas or water breakthrough occurs it interferes with production from other layers. The better strategy may be to drill multiple horizontal wells, each on strike and staying in a specific bed. The advantage to this strategy is that each of the wells is optimal in its standoff from the gas-oil or oil-water contact, thus delaying multiphase production as long as possible, and in its productive length within the formation, thus maximizing productivity.

1-7. Stimulation execution

A good understanding of job execution is necessary for making decisions on the applicability and risk of various treatments. As with any well work, basic safety procedures must be developed and followed to prevent catastrophic failure of the treatment, which could result in damage to or loss of the well, personnel and equipment. Specific standards and operating procedures have been developed for stimulation treatments, which if followed can lead to a safe, smooth and predictable operation. Chapters 11 and 19 fully detail execution concerns.

1-7.1. Matrix stimulation

Matrix stimulation, mainly acidizing, is the original and simplest stimulation treatment. More than 40,000 acid treatments are pumped each year in oil and gas wells. These treatments (Fig. 1-22) typically involve small crews and minimal equipment. The equipment usually consists of one low-horsepower, single-action reciprocating pump, a supply centrifugal and storage tanks for the acid and flush fluids. Blending equipment is used when solids are added to the treatment.

The most common process is for the fluids to be preblended at the service company facility and then transported to the location. This allows blending small volumes accurately, controlling environmental hazards. The fluids are then pumped with little effort or quality risk.

1-7.2. Hydraulic fracturing

Unlike matrix stimulation, fracturing can be one of the more complex procedures performed on a well (Fig. 1-23). This is due in part to the high rates and

Figure 1-22. Matrix stimulation treatment using a coiled tubing unit, pump truck and fluid transport.

pressures, large volume of materials injected, continuous blending of materials and large amount of unknown variables for sound engineering design.

The fracturing pressure is generated by single-action reciprocating pumping units that have between 700 and 2000 hydraulic horsepower (Fig. 1-24). These units are powered by diesel, turbine or electric engines. The pumps are purpose-built and have not only horsepower limits but job specification limits. These limits are normally known (e.g., smaller plungers provide a higher working pressure and lower rates). Because of the erosive nature of the materials (i.e., proppant) high pump efficiency must be maintained or pump failure may occur. The limits are typically met when using high fluid velocities and high proppant concentrations (+18 ppg). There may be numerous pumps on a job, depending on the design.

Mixing equipment blends the fracturing fluid system, adds the proppant and supplies this mixture to the high-pressure pumps. The slurry can be continuously mixed by the equipment (Fig. 1-25) or batch mixed in the fluid storage tanks. The batch-mixed fluid is then blended with proppant in a continuous stream and fed to the pumps.

Figure 1-23. This large fracturing treatment used 25,000 hydraulic horsepower and 1.54 million gal of fracturing fluid to place 6.3 million lbm of propping agent. The job lasted 11 hours.

Figure 1-24. *One thousand hydraulic horespower pumping unit.*

Figure 1-25. *For this fracturing treatment, propping agent was introduced into the fracturing fluid via conveyors to the blender. The blender added the propping agent to the continuously mixed fracturing fluid (creating a slurry) and discharged the slurry to the high-pressure pumping equipment.*